Energy Conversion and Management: X 20 (2023) 100436

Contents lists available at ScienceDirect

Energy Conversion and Management: X

journal homepage: www.sciencedirect.com/journal/energy-conversion-and-management-x

Techno-economic optimization of hybrid-electric power plants onboard cruise ships

A. Dotto [a,*], F. Satta [a]

[a] DIME, University of Genoa, via Montallegro 1, Italy

ARTICLE INFO

Keywords:
Hybrid-electric propulsion
Cruise ships
Liquefied Natural Gas
MILP
Energy
Environmental
Economic optimization

ABSTRACT

This work aims at assessing energy, environmental and economic performances of hybrid-electric plants installed onboard large-size cruise vessels fuelled by Liquefied Natural Gas. Specifically, hybrid-electric power plants coupling combined gas electric and steam plants, reciprocating engines and lithium-ion battery pack are considered. By adopting cogeneration efficiency, carbon dioxide emissions, nitrogen oxide emissions and costs as objective functions, optimal performances were assessed by a Mixed Integer Linear Programming code, following a two-step procedure. First, the MILP code has been applied considering 8-days long, phase-mean operating profiles to identify an optimal design of the engine room. Second, power plant performances have been investigated by applying MILP code to hourly demand profiles, in order to provide more detailed insight on working schedule. Overall, as main outcome of the phase-mean analysis, the potential of combined gas electric and steam plants and lithium-ion batteries in promoting a more efficient energy utilization, reduced environmental impact and enhanced cost savings is proved. Specifically, combined gas electric and steam plant was shown to optimize objective functions during navigation and maneuvering, whereas batteries improved energy and environmental performances in the most demanding ship operating conditions. Furthermore, optimal sizing of lithium-ion battery pack was determined at 40 MWh, despite its economic competitiveness resulted to deeply rely on carbon tax. On the other hand, the hourly analysis showed that controlling the combined gas electric and steam plant and batteries according to a mixed spinning reserve-peak shaving strategy optimizes the performance of power plant even in port conditions, with almost no role played by reciprocating engines. In detail, in comparison to a reference non-hybrid electric power plant, batteries are shown to improve cogeneration efficiency and greenhouse gas emission savings by nearly 2%, whereas nitrogen oxide emissions and costs were reduced by 12% and 2%, respectively.

1. Introduction

In the last few decades, even more demanding regulations concerning pollutant and greenhouse gas (GHG) emissions from ship power plants have been introduced within the maritime sector [1,2]. Owing to its reduced environmental and health impacts in comparison to HFO, Liquefied Natural Gas (LNG) is presently evaluated a viable option for the short-term decarbonization of shipping [3–5]. Furthermore, hybrid-electric power plants and highly-efficient Waste Heat Recovery (WHR) systems are recently receiving great attention to enable primary energy savings, especially for cruise vessels [6]. Since genetic algorithms retain nonlinear parameters (e.g., efficiencies) and effectively find out global minima, they were used by Ancona et al. [7] to minimize fuel consumption onboard a cruise ship dealing with a number of energy sources including electrical energy storage. Lan et al. [8] proposed a method for determining the optimal design of a stand-alone ship power plant including photovoltaic panels, diesel generator and batteries, aimed to minimize costs and CO_2 emissions. Misyris et al. [9] proposed a system identification method to estimate the state of charge (SOC) and capacity of the battery used onboard ships, whereas Dedes et al. [10] underlined the potential of 14% reduction in GHG emissions for hybrid battery-Diesel electric propulsion. Similarly, Vieira et al. [11] and Geertsma et al. [12] found out that further benefits on emissions can be achieved by adapting power plant configurations to specific mission profiles. Additionally, several works in the literature introduced specific control strategies, such as peak-shaving or spinning reserve, to increase battery life and reduce fuel consumption [13–16].

For what concerns the heat engine, it is well established in the energy production sector how combining a gas turbine (GT) with a bottoming

* Corresponding author.
E-mail address: alessandro.dotto@edu.unige.it (A. Dotto).

https://doi.org/10.1016/j.ecmx.2023.100436

Available online 20 August 2023
2590-1745/© 2023 The Author(s). Published by Elsevier Ltd. This is an open access article under the CC BY-NC-ND license (http://creativecommons.org/licenses/by-nc-nd/4.0/).

Nomenclature

$B3$	Set of boilers for 3 bar steam
$B9$	Set of boilers for 9 bar steam
$C^{el,ES}$	Maximum charge rate for batteries, W
$c^{el,ES}$	Minimum charge rate for batteries, W
C_{bat}	Battery capacity, Wh
$C_{max,bat}$	Maximum battery capacity, Wh
$CAux$	CAPEX of auxiliaries, €
CC	CAPEX cost for batteries, €/Wh
CC	Capital cost, €/W
CEM	Emission cost, €/s
CF	Fuel cost, €/kg
CG	Cost of electricity from the grid, €/s
CM	Maintenance cost, €/Wh
CRF	Capital Cost Recovery factor
CT	Carbon tax, €/kg
D	Power demand, W
$D^{el,ES}$	Maximum discharge rate for batteries, W
$d^{el,ES}$	Minimum discharge rate for batteries, W
$EEDI$	Energy Efficiency Design Index, $g_{CO_2}/(t * nm)$
Em	CO_2 emissions, g_{CO_2}
$Emno$	NO_x emissions, g_{NO_x}
F	Fuel consumption, kg/s
G	Set of COGES plants
LHV	Lower Heating Value, J/kg
P	Power, W
p	price, €
R	Set of reciprocating engines
S	Specific fuel consumption
T	Set of time intervals
V_{ref}	Reference ship speed
x	Logic variable
y	Logic variable

Greek symbols

Δt	Time interval, s
$\eta_{c,ES}$	Charge efficiency of batteries
$\eta_{d,ES}$	Discharge efficiency of batteries
η_{el}	Electrical efficiency
η_g	Cogeneration efficiency
γ	CO_2 emission factor, g_{CO_2}/g_{fuel}
π	Minimum power, W
Π	Maximum power, W
ξ	Conversion factor for emissions, g_{NO_x}/g_{CO_2}

Superscripts

el	Electrical power
$th3$	Thermal power at 3 bar
$th9$	Thermal power at 9 bar

Abbreviations

AP	Azipod
BT	Bow thruster
CAPEX	CAPital EXpenditure, €
COGES	COmbined Gas Electric and Steam
DF	Dual-Fuel
EES	Elecrical Energy Storage
EG	Electrical Generator
EM	Electrical Motor
GT	Gas Turbine
HRSG	Heat Recovery Steam Generator
OPEX	OPerational EXpenditure, €
RE	Reciprocating Engine
ST	Steam Turbine
WHR	Waste Heat Recovery

Subscripts

0	Related to nominal condition
$AC-DC$	Related to converters
AE	Related to auxiliary engine
b	Index on boilers
$B3$	Related to boilers for 3 bar steam
$B9$	Related to boilers for 9 bar steam
bat	Related to batteries
CH_4	Related to methane
CO_2	Related to carbon dioxide
el	Related to electrical power
ES	Related to energy storage
g	Index on COGES plants
LNG	Related to Liquefied Natural Gas
MDO	Related to Marine Diesel Oil
ME	Related to main engine
NO_x	Related to nitrogen oxide
r	Index on reciprocating engines
st	Related to fuel storage tanks
t	Index on time instants
$th3$	Related to thermal power at 3 bar
$th9$	Related to thermal power at 9 bar

steam power cycle presently offers the highest efficiencies among all available power plant technologies for sizes exceeding 10 MW [17]. For this reason, COmbined Gas Electric and Steam (COGES) plants based on aeroderivative GT were introduced in the marine sector during '70s. Merz and Pakula [18] were among the firsts to underline the benefits of GTs in terms of low environmental impact, reduced fuel consumption and increased operational flexibility, whereas Haglind [19] applied COGES to container ships, tankers and bulk carriers. Successive works assessed COGES plants installed on large container ships [20,21], whereas the high power-to-weight ratio provided by gas turbines determined the widespread use of GT engines in the military sector [22,23]. Recently, Dotto et al. [24–26] showed how integrated COGES-dual fuel (DF) engine power plants can provide benefits in terms of cogeneration efficiency over extremely flexible operating conditions for cruise-ferries. Moreover, also small-size COGES plants have been found to be a promising solution in the application onboard medium size cruise and Ropax ships [27–29]. Though COGES plants may offer high energy efficiency, low environmental impact and more volume onboard for passengers, only few cruise ships powered by these plants (i.e. Millennium and Infinity from Celebrity or Radiance of the Seas from the Royal Caribbean) were built in the past. Nevertheless, they appear promising for the decarbonization of the cruise ship industry. Recent environmental constraints imposed ship propulsion plant design and operation to change in a long-term perspective, aimed at identifying which technologies, and with which respective size, should be installed onboard.

The analogous problem of optimally designing and operating power plants arises from the polygeneration [30–32,14,33] and Combined Heat and Power (CHP) [34–36] fields. In the literature concerning distributed energy systems, Mixed-Integer Linear Programming (MILP) models are commonly adopted to face the short- and long-term planning, since the computational complexity of the problem is reduced by considering only linear relations, though actual and reliable results can be obtained. Wu et al. [36] developed a MILP model aimed to determine both optimal layout and operation strategy of distributed CHP systems,

by considering the annual capital, maintenance and operation costs as the objective function to be minimized. Similarly, a MILP model was developed by Mehleri et al. [37] to optimally design and operate a CHP energy system in a limited urban area and a residential district including micro-cogeneration units, photovoltaic panels and boilers. The optimal design of a polygeneration energy system for the Savona eco-campus was investigated in Bracco et al. [38] by means of a MILP model, which was able to account for various economic and/or environmental objective functions. Similarly, MILP program was used in Weber et al. [39] and Ren et al.[40] to study eco-town or eco-campus issues. Compared to genetic algorithms such as NSGA-II, MILP codes performing local linearization of nonlinear phenomena were shown to provide significant benefits in terms of computational costs [41–43]. Specifically, Ghaemi et al. [43] demonstrated that the MILP solver is able to optimize operation of district energy systems 2.5 times faster than genetic algorithms. Furthermore, implementing the MILP solver required fewer initial parameters than the NSGA-II method and ensured immediate check for constraint satisfaction. Interestingly, both MILP and genetic algorithms were shown to accurately find out the same global optimum condition, hence proving benefits from MILP also in this respect [43]. Nevertheless, different approaches from MILP are also present in the literature of distributed generation systems. Pruitt et al. [44] developed a model aimed to describe the part-load performance of components usually included within cogeneration plants by introducing non-linear constraints, with significant drawbacks in terms of complexity and computational cost compared to MILP strategy. Similarly, Gabrielli et al. [45] applied complex Mixed Integer Non-Linear Programming (MINLP) code for the optimal operation of the Polytechnic of Zurich, whereas a piecewise linear strategy was proposed by Coffrin et al. [46] to account for non-linearities in a computationally cost effective way.

Due to the even more strict environmental regulations [47–49], optimal design and scheduling of complex cruise ship power plants with accurate and computationally cheap tools are gaining importance in recent years. In this regard, few works in the literature are focused on the potential of MILP methods applied to hybrid-electric ship power plants [50]. Thus, to bridge this gap, the present work investigates the application of MILP codes for the optimal design and operation of hybrid-electric power plants onboard cruise ships. This work follows those previously carried out by the authors on the thermodynamic, environmental and economic analysis of integrated COGES-reciprocating engines plants onboard cruise ships [24–26,29,28,27], with the addition of batteries and of a new optimization approach as compared with previous analyses. With the aim of assessing the feasibility of battery installation onboard cruise ships and evaluating the optimal design of the power plant, MILP optimization is first performed considering phase-mean power demand profiles. Successively, once the power plant configuration is determined and the battery pack sized, MILP optimization has been applied to hourly power demand profiles, to gain a more detailed insight into the optimal scheduling of the power plant operation and its control strategy.

In detail, in Section 2 the MILP code is described with the aim of highlighting model assumptions and objective functions used, whereas Section 3 introduces the main characteristics of the cruise ship under study. In Section 4.1, energy-environmental-economic optimizations are performed considering phase-mean power demands and the optimal sizing of the battery pack is yielded. Finally, to gain a detailed insight on power supply, Section 4.2 performs the same energy-environmental-economic optimizations of Section 4.1 over a hourly demand profile.

2. Mathematical model

In this section, the Mixed-Integer Linear Programming model developed in the present work is introduced focusing on the main parameters as well as on the equations the algorithm relies on. As explained in Section 1, the code has been used in a twofold perspective. First, the number of battery modules has been retained variable, with the aim of finding out optimal sizing of the battery pack, i.e. the overall battery capacity enabling either maximum η_g for the power plant, minimum $CO_{2,eq}$ emissions, minimum NO_x emissions or minimum costs. To lower the computational cost at this first stage, the analysis has been carried out on phase-mean operational profiles for both ship and engine room. Second, by adopting the optimal size of the battery pack found within the phase-mean analysis, the energy, environmental and economic performances of the hybrid-electric power plant have been optimized considering hourly operational profiles, for the same objective functions previously used (i.e., $\eta_g, CO_{2,eq}, NO_x$ and costs). Thus, due to hourly time discretization, the second step of the procedure aims to address optimal scheduling of the power plant with more details. In Fig. 1, a diagram summarising the overall architecture of the MILP code is introduced for sake of clarity. In detail, all the operational decision variables and constraints implemented are shown for each component, together with the definition of the objective functions considered. By a numerical point of view, the model uses linear relations when linear functional dependency exists between two variables (e.g., relation between electrical power of prime movers and their working load). Instead, when non-linear functional dependency exists (e.g., dependency of the electrical efficiency of prime movers from their working load), piece-wise linear relations are considered over specific discretization grid. Furthermore, as can be seen in Fig. 1, some logic variables (e.g., x and y) are used in the model to represent the turned on/turned off conditions of prime movers and boilers as well as their inclusion onboard. In the following, variables and equations implemented within the model are introduced in detail, adopting a classification approach based on functional use.

2.1. Inputs

Three main types of input data are considered. Firstly, general data accounting for various power plant configurations are considered. Specifically, they represent the type and number of prime movers which may be included within the power plant or the variable time-step sampling used in computing the solution:

- G: set of COGES plants included within the ship power plant
- R: set of dual-fuel or natural gas reciprocating engines included within the ship power plant
- $B9$: set of MDO-fuelled boilers included within the ship power plant to cover the thermal power demand at 9 bar
- $B3$: set of MDO-fuelled boilers included within the ship power plant to cover the thermal power demand at 3 bar
- T: set of time intervals t the considered horizon consists in, each characterized by a specific and potentially variable time extension Δt

Secondly, technical data are necessary to correctly represent component performances and characteristics (delivered power, efficiency, fuel consumption, emissions, volumes, weights,…):

- $D_t^{el}, D_t^{th9}, D_t^{th3}$: electrical and thermal power demands at time t. The thermal power is distinguished depending on the steam pressure required (3 or 9 bar), whereas D_t^{el} accounts for both propulsion and hotel electrical loads, as more in depth described in Dotto et al. [25].
- $\pi_g^{el,G}, \Pi_g^{el,G}$: minimum and maximum electrical power potentially provided by COGES. The maximum value considered corresponds to 97% load such that a 3% Engine Margin (EM) is accounted for. The electrical power delivered at 50% load is taken as the minimum limit, since COGES efficiency drastically reduces under this threshold, according to the findings of previous analyses carried out by the authors [24,26].
- $\pi_g^{th3,G}, \Pi_g^{th3,G}, \pi_g^{th9,G}, \Pi_g^{th9,G}$: minimum and maximum thermal power potentially provided by COGES at 3 and 9 bar, respectively. The

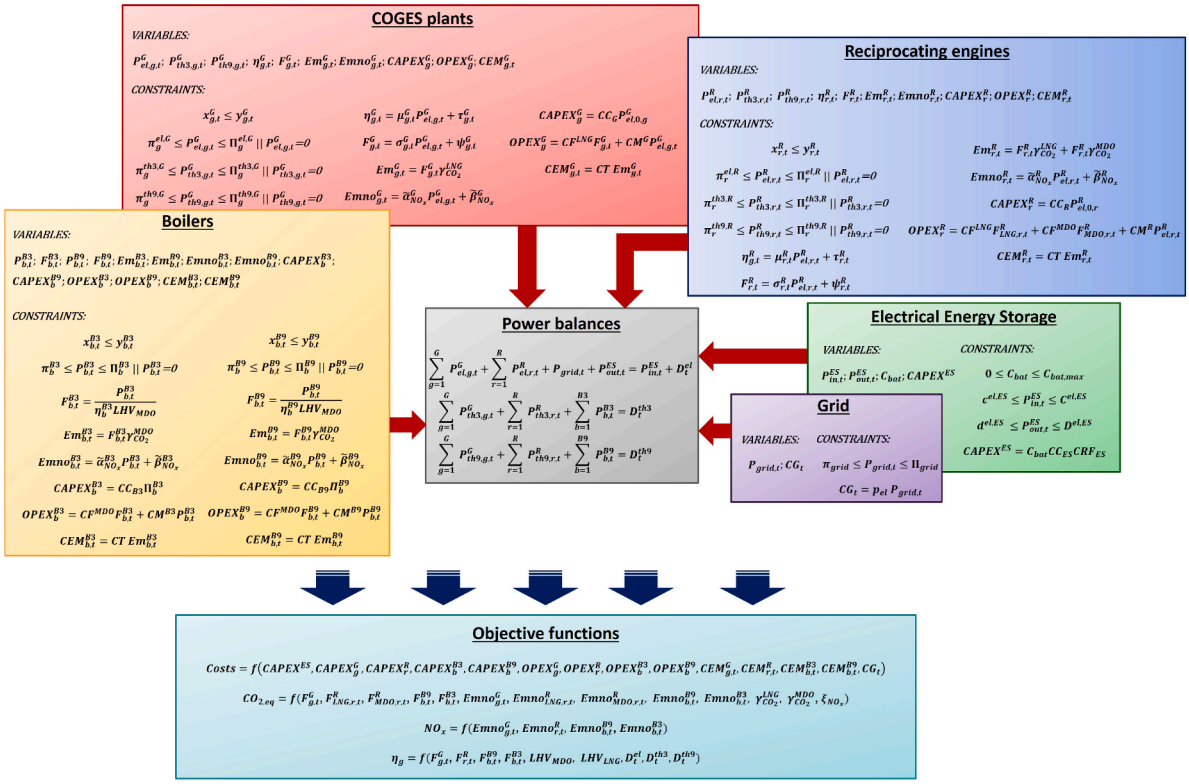

Fig. 1. Sketch of the overall architecture of the MILP code. Decision variables and constraints are shown for each power source. Global constraints (i.e. power balances) and objective functions in which the variables are involved are also reported.

thermal power at 9 bar is provided through steam extraction from the steam turbine, whereas steam at 3 bar is available from the discharge of the steam turbine, considering a back-pressure configuration, as discussed in detail in Dotto et al. [25].

- $\pi_r^{el,R}$, $\Pi_r^{el,R}$: minimum and maximum electrical power provided by reciprocating engines. The maximum value considered corresponds to 90% load such that a typical 10% EM is accounted for, whereas $\pi^{el,R}$ is taken at 40% load, according to previous authors' analyses [24,26].
- $\pi_r^{th3,R}$, $\Pi_r^{th3,R}$, $\pi_r^{th9,R}$, $\Pi_r^{th9,R}$: minimum and maximum thermal power provided by reciprocating engines at 3 and 9 bar, respectively. The thermal power at 9 bar is provided by the high temperature (HT) circuit, whereas steam at 3 bar can be generated from lubrication and cooling circuits. Only the WHR of large-size engines are considered, since small-size engines are not able to provide significant thermal power, as found in a previous authors' analysis [24].
- $\mu_{g,t}^G$, $\tau_{g,t}^G$, $\mu_{r,t}^R$, $\tau_{r,t}^R$: coefficients used for local linearization of the efficiency curves of GTs and reciprocating engines in function of the percentage load. Instead, the dependency of GTs performance from the ambient temperature is accounted for in a fully nonlinear way, based on curves available in the literature from the manufacturers.
- $\sigma_{g,t}^G$, $\psi_{g,t}^G$, $\sigma_{r,t}^R$, $\psi_{r,t}^R$: linearization coefficients applied to the fuel consumption curves of GTs and reciprocating engines, respectively.
- $P_{el,0,g}^G$, $P_{el,0,r}^R$: electrical power delivered by COGES plant g and reciprocating engine r at 100% load.
- π_b^{B3}, π_b^{B9}: minimum thermal power provided by boilers generating steam at 3 and 9 bar, respectively.
- Π_b^{B3}, Π_b^{B9}: maximum thermal power provided by boilers generating steam at 3 and 9 bar, respectively.
- η_b^{B3}, η_b^{B9}: efficiencies of boilers generating steam at 3 and 9 bar, respectively.
- LHV: fuel lower heating value
- $d^{el,ES}$, $D^{el,ES}$: minimum and maximum discharge rate for the electrical energy storage, respectively
- $c^{el,ES}$, $C^{el,ES}$: minimum and maximum charge rate for the electrical energy storage, respectively
- $N_{bat,max}$, N_{bat}: maximum and currently installed number of batteries within the electrical storage system
- $C_{bat,max}$, C_{bat}: maximum and current capacity of the electrical storage system
- $\eta_{d,ES}$, $\eta_{c,ES}$: discharge and charge efficiency of the electrical energy storage
- π_{grid}, Π_{grid}: minimum and maximum electrical power withdrawable from the harbour grid in Cold Ironing (CI) condition
- $\gamma_{CO_2}^{LNG}$, $\gamma_{CO_2}^{MDO}$: CO_2 emission factor for LNG and MDO
- $\tilde{\alpha}_{NO_x}^G$, $\tilde{\beta}_{NO_x}^G$, $\tilde{\alpha}_{NO_x}^R$, $\tilde{\beta}_{NO_x}^R$, $\tilde{\alpha}_{NO_x}^{B3}$, $\tilde{\beta}_{NO_x}^{B3}$, $\tilde{\alpha}_{NO_x}^{B9}$, $\tilde{\beta}_{NO_x}^{B9}$: correlation coefficients used for computing the NO_x emissions from GTs, reciprocating engines, boilers producing steam at 3 bar and boilers producing steam at 9 bar

Thirdly, cost data necessary to perform economic optimization are provided to the MILP program:

- CC_G, CC_R, CC_{B9}, CC_{B3}: power specific CAPital EXpenditure (CAPEX) for purchasing GTs, reciprocating engines, boilers producing steam at 9 bar or 3 bar, respectively. For sake of clarity, the corresponding values used in the present work are reported in Table 1, following previous works available in the literature [51,24,52].
- CC_{EM}, CC_{EG}, CC_{AC-DC}, CC_{st}: power specific CAPital EXpenditure (CAPEX) for purchasing electrical motors, electrical generators, AC-DC or DC-AC converters and fuel storage tank, respectively (see Table 1), whose values have been chosen following previous works available in the literature [51,24,52].

Table 1
Power specific and energy specific CAPEX costs of power plant components used to compute overall investment costs [51,24,52].

COMPONENT	CAPEX
Reciprocating engines [€/kW]	365–420
Gas Turbines [€/kW]	380
Li-ion batteries [€/kWh]	200
HRSG + ST [€/kW]	127
Tanks [€/kWh]	0.94
Electrical Generators [€/kW]	90
Electrical Motors [€/kW]	80
AC/DC-DC/AC converters [€/kW]	100
Propellers [€/kW]	30

Table 2
Economical values used for computing fuel, maintenance and emission costs [60,52,61,62,51].

COMPONENT	OPEX
LNG fuel [€/t]	398
MDO fuel [€/t]	575
Reciprocating engine OM [€/kWh]	0.015
COGES OM [€/kWh]	0.002
Boiler OM [€/kWh]	0.006
CO_2 price [€/kg]	0.115

- CF^{LNG}, CF^{MDO}: fuel costs in €/t for LNG and MDO, respectively, used for OPEX computation (see Table 2), as discussed in detail by Dotto et al. [24]
- ξ_{NO_x}: conversion factor used to transform NO_x emissions into CO_2 equivalent emissions, according to Lammel and Grassl [53]
- $CM^G, CM^R, CM^{B9}, CM^{B3}$: maintenance costs for COGES plants, reciprocating engines and boilers, respectively, used for OPEX computation (see Table 2)
- p_{el}: electricity purchasing price for Cold-Ironing (CI) in €/MWh. Specifically, the current price adopted for middle-large users in the ports of Spain and Sweden is considered, following previous works available in the literature [54–56]
- CRF: capital cost recovery factor assumed equal for GTs, reciprocating engines and boilers. A 20 years useful life and a 6% discount rate were adopted for traditional components, following the literature [57,24]
- CRF_{ES}: capital cost recovery factor for the electrical energy storage (i.e. Li-ion batteries). For batteries, a 15 years useful life was assumed to take into account performance reduction [58], and a discount rate of 6% was used.
- CT: carbon tax due to CO_2 emissions, estimated from the early-future policies and intentions in EU following the work of Perić et al. [52].
- CC_{ES}: investment cost for the electrical energy storage system, assumed equal to 200 €/kWh (see Table 1), as previoulsy found by Lehmusto and Santasalo-Aarnio [59].

2.2. Decision variables

Two main types of decision variables are accounted for in the MILP program. Specifically, binary variables are used to model the inclusion/exclusion of components as well as their working or turned-off condition in a certain time interval [35]:

- $y_g^G, y_r^R, y_b^{B3}, y_b^{B9}$: equal to 1 in case COGES g, reciprocating engine r and 3-bar/9-bar boilers b are installed onboard, respectively
- y^{ES}: equal to 1 in case batteries are installed onboard
- $x_{g,t}^G, x_{r,t}^R, x_{b,t}^{B3}, x_{b,t}^{B9}$: equal to 1 in case COGES g, reciprocating engine r and 3-bar/9-bar boilers b are turned on at a certain time t, respectively
- x_t^{ES}: equal to 1 in case batteries are working at time t in charging or discharging mode

Then, operational decision variables provide the performance of working components at each time t:

- $P_{el,g,t}^G, P_{th3,g,t}^G, P_{th9,g,t}^G, \eta_{g,t}^G, F_{g,t}^G$: electrical power and thermal power (at 3 or 9 bar), electrical efficiency and LNG fuel consumption, delivered from the COGES plant g at time t, respectively
- $P_{el,r,t}^R, P_{th3,r,t}^R, P_{th9,r,t}^R, \eta_{r,t}^R, F_{LNG,r,t}^R, F_{MDO,r,t}^R$: electrical power and thermal power (at 3 or 9 bar), electrical efficiency, LNG fuel consumption and MDO fuel consumption generated by the reciprocating engine r at time t, respectively
- $P_{b,t}^{B3}, P_{b,t}^{B9}$: thermal power generated by the 3-bar and 9-bar boilers b at time t, respectively
- $F_{b,t}^{B3}, F_{b,t}^{B9}$: MDO fuel consumption required by the 3-bar and 9-bar boilers b at time t, respectively
- $P_{in,t}^{ES}, P_{out,t}^{ES}$: charging and discharging electrical power for the energy storage system at time t, respectively
- $P_{grid,t}$: electrical power withdrawn from the harbour grid due to cold ironing at time t
- $OPEX_{g,t}^G, OPEX_{r,t}^R, OPEX_{b,t}^{B3}$ and $OPEX_{b,t}^{B9}$: OPerational EXpenditure (OPEX) caused by fuel consumption and maintenance costs concerning the COGES plant g, reciprocating engine r and boilers b working at time t.
- $Em_{g,t}^G, Em_{r,t}^R, Em_{b,t}^{B3}$ and $Em_{b,t}^{B9}$: CO_2 emissions concerning the COGES plant g, reciprocating engine r and boilers b working at time t
- $CEM_{g,t}^G, CEM_{r,t}^R, CEM_{b,t}^{B3}$ and $CEM_{b,t}^{B9}$: costs due to carbon taxation for the CO_2 emissions concerning the COGES plant g, reciprocating engine r and boilers b working at time t
- CG_t: cost related to electrical power withdrawn from the harbour grid due to cold ironing at time t
- $Emno_{g,t}^G, Emno_{LNG,r,t}^R, Emno_{MDO,r,t}^R, Emno_{b,t}^{B3}, Emno_{b,t}^{B9}$: NO_x emissions concerning the COGES plant g, reciprocating engine r and boilers b working at time t [63,64]. Subscripts for NO_x emissions generated by reciprocating engines are distinguished for LNG and MDO fuels.

2.3. Objective functions

In this work, multiple optimization procedures have been assessed for a typical cruise ship power demand. Specifically, the optimization algorithms considered and their corresponding objective functions are the following [35,65]:

- Energy optimization: the algorithm consists of maximizing the power plant cogeneration efficiency, defined as

$$\eta_g = \frac{N}{D} \quad where \quad N = \sum_{t=1}^{T}(D_t^{el} + D_t^{th9} + D_t^{th3})\Delta t$$
$$D = \sum_{t=1}^{T}\left[\sum_{g=1}^{G} F_{g,t}^G LHV_{CH_4} + \sum_{r=1}^{R} F_{LNG,r,t}^R LHV_{CH_4} + \sum_{r=1}^{R} F_{MDO,r,t}^R LHV_{MDO} + \sum_{b=1}^{B9} F_{b,t}^{B9} LHV_{MDO} + \sum_{b=1}^{B3} F_{b,t}^{B3} LHV_{MDO}\right]\Delta t \quad (1)$$

- Environmental optimization: it consists of minimizing CO_2-equivalent emissions from the entire power plant

$$\begin{aligned} Total\ CO_2 \quad = & \sum_{t=1}^{T}\Bigg[\sum_{g=1}^{G}(F_{g,t}^{G}\gamma_{CO_2}^{LNG}+Emno_{LNG,g,t}^{G}\xi_{NO_x})+ \\ & \sum_{r=1}^{R}(F_{LNG,r,t}^{R}\gamma_{CO_2}^{LNG}+Emno_{LNG,r,t}^{R}\xi_{NO_x})+ \\ & \sum_{r=1}^{R}(F_{MDO,r,t}^{R}\gamma_{CO_2}^{MDO}+Emno_{MDO,r,t}^{R}\xi_{NO_x})+ \\ & \sum_{b=1}^{B9}(F_{b,t}^{B9}\gamma_{CO_2}^{MDO}+Emno_{b,t}^{B9}\xi_{NO_x})+ \\ & \sum_{b=1}^{B3}(F_{b,t}^{B3}\gamma_{CO_2}^{MDO}+Emno_{b,t}^{B3}\xi_{NO_x})\Bigg]\Delta t \end{aligned} \tag{2}$$

In order to assess differences between CO_2 and NO_x emissions generated, the overall nitrogen oxide emissions minimization is also performed by means of the following objective function:

$$\begin{aligned} Total\ NO_x \quad = & \sum_{t=1}^{T}\Bigg[\sum_{g=1}^{G}Emno_{LNG,g,t}^{G}+\sum_{r=1}^{R}Emno_{LNG,r,t}^{R}+ \\ & \sum_{r=1}^{R}Emno_{MDO,r,t}^{R}+\sum_{b=1}^{B9}Emno_{b,t}^{B9}+ \\ & \sum_{b=1}^{B3}Emno_{b,t}^{B3}\Bigg]\Delta t \end{aligned} \tag{3}$$

It is well known in the maritime sector how new ships must comply with IMO regulations concerning the Energy Efficiency Design Index (EEDI), which limits CO_2 emission levels. In this work, parallel to the above optimization algorithms, the EEDI index compliance is investigated. EEDI definition from IMO is reported in eq. (4) [66,24]:

$$\begin{aligned} EEDI \quad = & \frac{\prod_{j=1}^{n}f_j\sum_{i=1}^{n_{ME}}P_{ME_i}\gamma_{ME_i}S_{ME_i}}{f_if_cCapacityf_wV_{ref}}+ \\ & \frac{\prod_{j=1}^{n}f_j\sum_{i=1}^{n_{AE}}P_{AE_i}\gamma_{AE_i}S_{AE_i}}{f_if_cCapacityf_wV_{ref}}+ \\ & \frac{\sum_{i=1}^{n_{eff}}f_{eff_i}P_{eff_i}\gamma_{ME}S_{ME}}{f_if_cCapacityf_wV_{ref}} \end{aligned} \tag{4}$$

where S is the specific fuel consumption, P indicates power, n is number of engines and γ consists in the CO_2 emission factor depending on fuel molecules. The subscripts ME, AE and eff refer to main engines, auxiliary engines and innovative energy technologies (i.e. batteries or steam bottoming cycle), respectively. Since in integrated-electric power plants no distinction arises between ME and AE, only terms concerning main engines are accounted for. Finally, the values for f_{eff}, f_i, f_j, f_c and f_w factors can be assessed by consulting IMO regulations [67].

- Economic optimization: it coincides with minimizing overall costs for the design and operation of the ship power plant. Three main variants are considered for this study, in order to better appreciate the benefits of hybrid-electric power plants onboard cruise ships: no carbon tax imposed and no cold ironing available; carbon tax imposed without the availability of cold ironing; carbon tax imposed and cold ironing available in harbour. Nevertheless, the most complete objective function for the economic optimization can be written as:

$$\begin{aligned} Total\ Costs \quad = & C_{bat}CC_{ES}CRF_{ES}+\sum_{g=1}^{G}\Big[CC_GP_{el,0,g}^{G}CRF\Big]+ \\ & \sum_{r=1}^{R}\Big[CC_RP_{el,0,r}^{R}CRF\Big]+\sum_{b=1}^{B9}\Big[CC_{B9}\Pi_b^{B9}CRF\Big]+ \\ & \sum_{b=1}^{B3}\Big[CC_{B3}\Pi_b^{B3}CRF\Big]+\sum_{t=1}^{T}\Bigg[\sum_{g=1}^{G}F_{g,t}^{G}CF_{CH_4}+ \\ & \sum_{r=1}^{R}F_{LNG,r,t}^{R}CF_{CH_4}+\sum_{r=1}^{R}F_{MDO,r,t}^{R}CF_{MDO}+ \\ & \sum_{b=1}^{B9}F_{b,t}^{B9}CF_{MDO}+\sum_{b=1}^{B3}F_{b,t}^{B3}CF_{MDO}\Bigg]\Delta t+ \\ & \sum_{t=1}^{T}\Bigg[\sum_{g=1}^{G}P_{el,g,t}^{G}CM^{G}+\sum_{r=1}^{R}P_{el,r,t}^{R}CM^{R}+ \\ & \sum_{b=1}^{B9}P_{thB,b,t}^{B9}CM^{B9}+\sum_{b=1}^{B3}P_{thB,b,t}^{B3}CM^{B3}\Bigg]\Delta t+ \\ & \sum_{t=1}^{T}\Bigg[\sum_{g=1}^{G}CEM_g^{G}+\sum_{r=1}^{R}CEM_r^{R}+ \\ & \sum_{b=1}^{B9}CEM_b^{B9}+\sum_{b=1}^{B3}CEM_b^{B3}\Bigg]\Delta t+ \\ & \sum_{t=1}^{T}CG_t\Delta t+CAux \end{aligned} \tag{5}$$

where $CAux$ summarises all the CAPEX costs for auxiliaries (e.g., electrical motors, propellers, fuel storage tanks, …), which have been evaluated considering a 20 years useful life and a 6% discount rate, according to other works reported in the literature [51,24,52].

Overall, these optimization studies are performed in a two-step procedure. Firstly, they are applied to 8-days phase-mean operating profiles for real cruise ships in order to investigate the technical, economical and environmental performance over a long-term horizon. Then, the same optimization procedures are applied on a representative hourly profile covering 48 h, in order to assess the short-term performance of the hybrid-electric power plant. Thus, a detailed view of the benefits and operation strategies of electrical energy storage systems is provided for a short- and long-term planning.

2.4. Problem constraints

Where electrical and thermal power supply at each t is concerned, constraints aimed at considering only installed prime movers and boilers among all the available components are introduced. Furthermore, the electrical and thermal power delivered by prime movers or boilers are constrained to be comprised between their minimum and maximum values. Piecewise linearization of efficiency and fuel consumption curves for COGES plant and reciprocating engines has been assumed [68,69], while well-established correlations for computing NO_x emissions generated by prime movers and boilers have been considered [70,63,71]. Finally, constraints for cost computation have been imposed. All the numerical expressions used for constraints are reported in the appendix 6 for clarity.

3. Case study

In this work, the performance of a hybrid-electric power plant installed onboard a 114000 Gross Tonnage, 3780 passengers cruise ship sailing in the Mediterranean Sea is investigated. Specifically, an integrated electric power plant including COmbined Gas Electric and Steam, Electric Energy Storage system (EES), Dual-Fuel (DF) and Natural Gas (NG) reciprocating engines is applied, as schematically shown in Fig. 2.

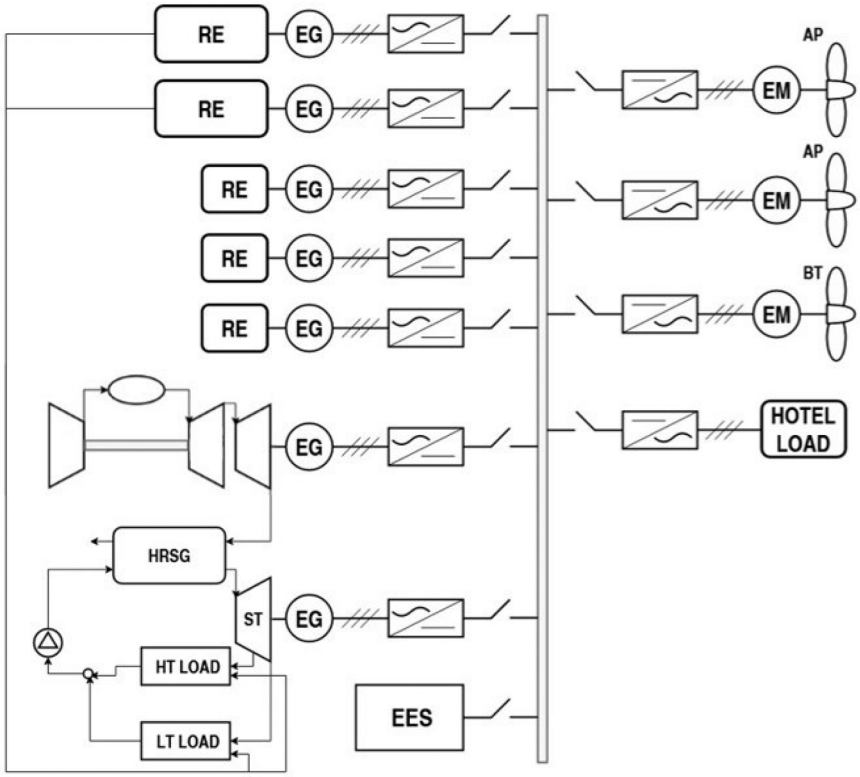

Fig. 2. Schematic view of power plant investigated for cruise ship.

Table 3
Electrical and thermal power requests in MW for hotel services.

Power demand	Phase	S	W
	Navigation	21.262	24.822
LT	Port	10.937	14.327
	Navigation	1.784	1.784
HT	Port	1.784	1.784
	Navigation	9.962	9.090
P_{hotel}	Port	8.704	7.504

Electric and thermal power demands during navigation, port and maneuvering conditions have been built considering data available in the literature for cruise ships dealing with comparable Gross Tonnage and passenger number. In details, the cubic curve (V_{ship}, P_o) reported in Gualeni et al. [72] and based on actual experimental data is used to gain the power demand requested for propulsion. On the other hand, the hotel electrical power demand existing during port and navigation conditions has been estimated according to Armellini et al. [65] and is reported in Table 3, distinguishing summer and winter seasons. Table 3 clearly shows how electrical power request during navigation is slightly higher than at berth conditions, due to the power needed by auxiliary systems related to the propulsion chain [72]. On the other hand, power demand for air conditioning in cabins mainly determines variations with season. Where the electrical power demand during maneuvering is concerned, estimating it in accurate way represents a particularly challenging issue due to its dependency on local climatic conditions, port layout and master's expertise. Towards this end, in this work the main engines (ME) and auxiliary engines (AE) have been considered turned on at 20% and 75% load, respectively, according to Meyer et al. [73] and Tzannatos [74]. Where thermal power demand onboard is concerned, the Low Temperature (LT) and High Temperature (HT) users have been considered. Specifically, the LT power demand deriving from both accommodation and production of fresh water (FW) by multi-stage evaporators is supplied by steam at 3 bar, whereas the HT power request is only needed by accommodation (sanitary water, swimming pools water, galley and laundry services) and is supplied by steam at 9 bar. In order to estimate the LT power demand, a 1000 m^3/day fresh water need has been assumed [75], whereas the portion of LT demand required from accommodation of large-size cruise ships has been derived from Armellini et al. [65]. On the other hand, a 1.784 MW HT power request accounting for accomodation users, in both summer and winter seasons, has been estimated (see Table 3) [76,77].

Where power demand profiles are concerned, a typical route for large MSC and Costa cruise ships in Mediterranean Sea has been considered, whose details in terms of locations, duration and ship speeds are reported in Table 4. Two different studies have been analysed. First, the power plant performance on the entire ship journey is investigated considering mean values for power demand during each ship operating condition (port, navigation or maneuvering). The phase-mean electrical and thermal power demand profiles which correspond to the route under consideration are shown in Fig. 3, for both summer and winter seasons. The x-axis indicates the ship operating phase for port (P) and navigation (N) conditions, whereas no symbol is added for maneuvering between each N and P phase to facilitate reading (see Table 4 for relevant parameters of the route).

Second, the power plant performances have been assessed considering hourly power demand profiles, which overall account for two days of the journey to limit computational cost. Specifically, the first two days, i.e. centered around the Genoa-Civitavecchia and Civitacchia-Palermo routes, have been considered as reference. The shapes of hourly fluctuations of the hotel loads, as well as those of the LT thermal power demand, have been derived from the experimental data acquired onboard a large-size cruise ship [78]. Finally, the HT power demand is considered fixed during the entire two days simulated. All the shapes of daily profiles have been scaled with the time-mean values reported in Table 3, in order to conserve the energy request amount over each ship operating condition. On the other hand, hourly variations of the propulsion power demand have been derived considering the actual ship

Table 4
Details of the Mediterranean route analysed (N = navigation, P = port, M = maneuvering).

LOCATION	PHASE	t [h]	V_{ship} [knots]
Genoa	M	0.5	0
Genoa-Civitavecchia	N	13	15
Civitavecchia	M	0.5	0
Civitavecchia	P	10	0
Civitavecchia	M	0.5	0
Civitavecchia-Palermo	N	15	17
Palermo	M	0.5	0
Palermo	P	7	0
Palermo	M	0.5	0
Palermo-Malta	N	16	18
Malta	M	0.5	0
Malta	P	8	0
Malta	M	0.5	0
Malta-Barcelona	N	38	18
Barcelona	M	0.5	0
Barcelona	P	10	0
Barcelona	M	0.5	0
Barcelona-Marseille	N	13	15
Marseille	M	0.5	0
Marseille	P	8	0
Marseille	M	0.5	0
Marseille-Genoa	N	14	16
Genoa	M	0.5	0

4. Results

4.1. Optimization procedures applied to phase-mean demand profiles

In this section, the optimization of the hybrid-electric power plant is performed considering time-mean electrical and thermal power requests over each ship operating condition (i.e. navigation, port, maneuvering). Specifically, η_g, $CO_{2,eq}$, NO_x and cost optimization algorithms introduced in Section 2 have been set up distinguishing winter and summer seasons. As main outputs, the thermal and electrical power delivered by prime movers to optimally cover demands in each ship operating condition is determined, together with the overall values achieved by objective functions. Furthermore, the size of the EES is considered variable in this section, hence optimal sizing of batteries is performed within all the energy management strategies. Specifically, the number of 20 kWh Li-ion batteries has been kept variable over the range 0–2000, thus the economic feasibility of including a battery pack onboard is also assessed.

Where the phase-mean profiles are concerned, Fig. 6 shows the electrical power delivered by prime movers in case of η_g (Fig. 6a), $CO_{2,eq}$ (Fig. 6b), NO_x (Fig. 6c) and cost (Fig. 6d) optimizations. The power demand is depicted in black, dotted line. Furthermore, since results for summer are qualitatively analogous, only results concerning winter are reported. Independently from the objective function considered, Fig. 6 shows how COGES plant supplies most of power during maneuvering

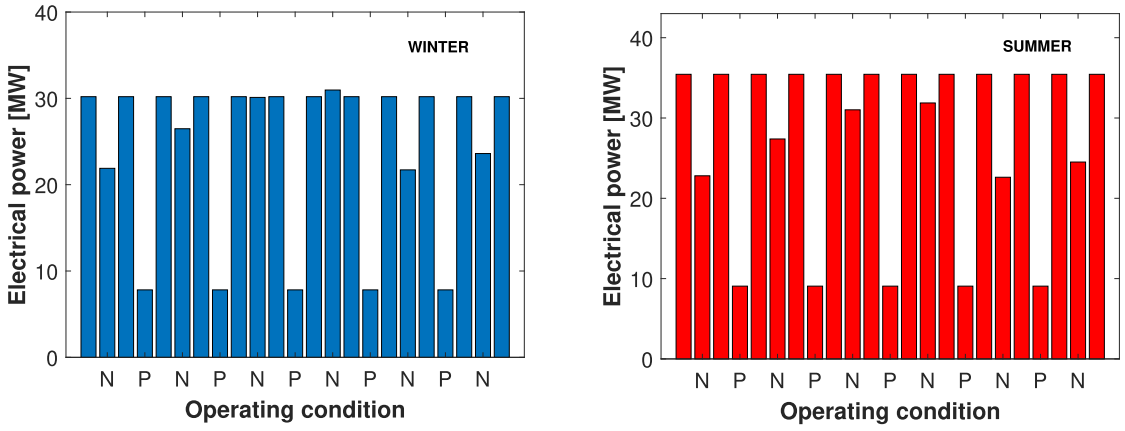

Fig. 3. Electrical power demand for phase-mean analysis (N = navigation, P = port). Labels for maneuvering, occurring between navigation and port operating conditions, have been omitted to improve the clearness of abscissa reading.

speed profile within the Genoa-Civitavecchia-Palermo route, obtained from marine traffic online platforms.

Fig. 4 shows the hourly profiles of electrical power demand requested onboard during the route considered, for both summer and winter seasons. Specifically, the cumulative plot for electrical power demand is shown in blue bar, the sum of hotel and maneuvering power demands is shown in yellow and, finally, the propulsion power request is depicted in orange. Instead, Fig. 5 shows the hourly profiles of HT (red) and LT (yellow) thermal power demands onboard during the considered route, for both summer (right) and winter (left) seasons.

Table 5 reports the main characteristics of prime movers considered. The power plant configuration adopted for the present study comprises one LM2500 gas turbine, two 9LMAN51/60 DF MAN engines and three R-R Bergen C26L9 natural gas reciprocating engines, used as small size electrical generators. Specifically, the LM2500 GT is considered coupled with a bottoming steam power plant in a COGES configuration based on back-pressure steam turbine. It should be remarked that the selected power plant configuration allows completion of the maneuvering phase even in the event of a failure of the largest prime mover, complying with regulation requirements [79].

and navigation, whereas reciprocating engines cover demand at berth. Focusing the attention on the η_g optimization (i.e. Fig. 6a), the Li-ion battery pack contributes to cover electrical power demand in almost all maneuvering and port operating conditions (e.g. see maneuvering phases during departure from Genoa and arrival to Civitavecchia ports and the berth conditions at Civitavecchia and Palermo ports, highlighted by red squares in Fig. 6a). Power delivered from the battery pack during maneuvering ranges from 3 to 10 MW and helps COGES plant to efficiently cover the entire demand. Specifically, for the electrical power range required during maneuvering, COGES plant coupled with batteries is able to provide the highest cogeneration efficiency of the power plant. On the other hand, batteries coupled with DF engines provide benefits in terms of energy savings during port conditions, where 2 MW power is provided by the energy storage system. Overall, for both maneuvering and port conditions, the high discharging efficiency of batteries increases η_g, despite prime movers run at part-loads. On the other hand, charging mode for batteries is enabled during few navigation conditions, along the routes Genoa-Civitavecchia, Civitavecchia-Palermo and Barcelona-Marseille. Since navigation involves the majority of time during the cruise, small amount of power is required to completely charge batteries. Furthermore, since excess power with

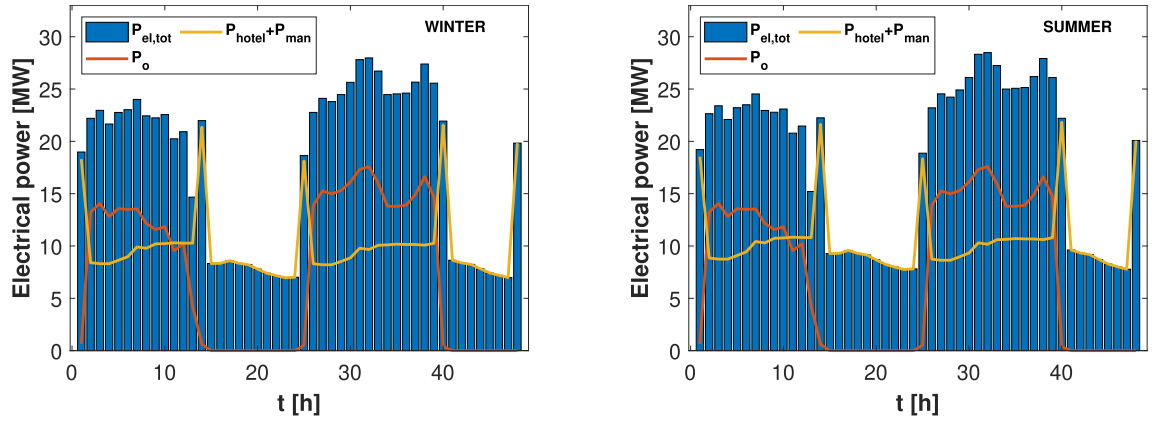

Fig. 4. Electrical power hourly distribution. P_o indicates the propulsion power during navigation, P_{man} the propulsion power requested during maneuvering, P_{hotel} the power demand from hotel services and $P_{el,tot}$ the overall electrical power demand (i.e. $P_{el,tot} = P_o + P_{man} + P_{hotel}$).

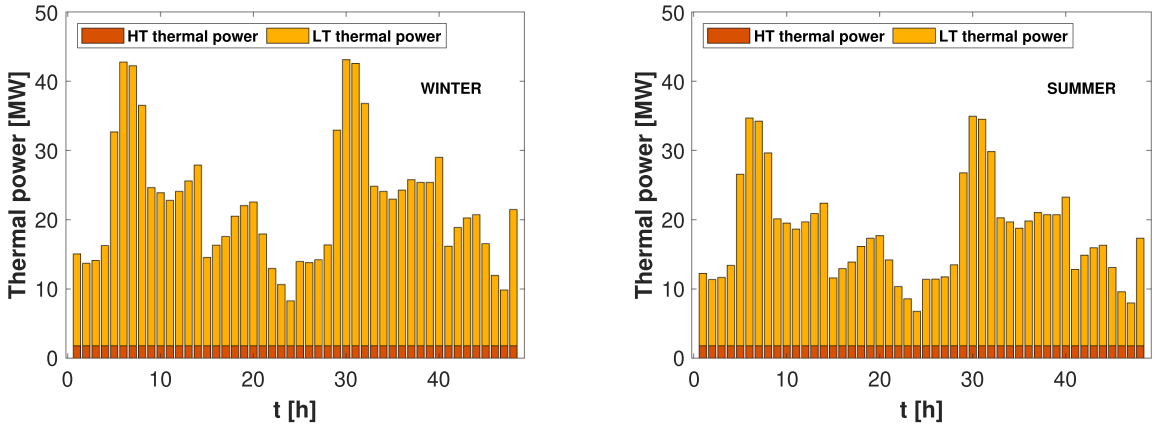

Fig. 5. Thermal power hourly distribution for winter (left) and summer (right) seasons.

Table 5
Prime mover main characteristics.

GT	P_{net} [MW]	$\eta_{el,GT}$ [%]	T_{ex} [°C]
LM2500	25.06	37	566
9L MAN 51/60	8.42	45.5	309
R-R Bergen C26L9	2.33	45	-

respect to demand is required to charge batteries, COGES plant works at higher loads (i.e. efficiency) with benefits in terms of cogeneration efficiency and energy savings. A further charging phase occurs in the last maneuvering, where additional power from NG engines is required to store energy into batteries, since COGES plant is running at maximum load. Interestingly, the charging phase of EES is positioned during ship operating conditions which are characterized by high cogeneration efficiency even in absence of batteries, whereas discharging mode occurs where the energy saving is lower. Thus, batteries appear to increase cogeneration efficiency both during charging and discharging phases. Comparing Figs. 6a and 6b shows how $CO_{2,eq}$ and η_g optimizations provide the same results, as expected. Indeed, for a fixed electrical and thermal power demand, maximizing η_g consists in minimizing the fuel consumption from prime movers. Thus, except for small affection on $CO_{2,eq}$ played by different emission factors of MDO and LNG and by higher NO_x produced by reciprocating engines in comparison with COGES, minimizing fuel consumption nearly coincides with minimizing $CO_{2,eq}$. Indeed, MDO used by DF engines is only 2% of the overall fuel consumption [5] and NO_x emissions are negligible with respect to CO_2 ones.

In case NO_x emissions, and their minimization, are considered independently from carbon dioxide ones, Fig. 6c shows power distribution provided by the optimization process. Results in Fig. 6c locally differ from those obtained from η_g and $CO_{2,eq}$ optimizations. Specifically, power withdrawn from batteries is more frequently used to help COGES during maneuvering and more energy is stored into batteries from COGES during navigation conditions. Furthermore, minimizing NO_x production avoids to discharge batteries in some port operating conditions in favour of NG engines. Both DF and NG engines covering power demand at berth are turned on at reduced loads when NO_x reduction is pursued in comparison to η_g and $CO_{2,eq}$ optimizations reported in Figs. 6a and 6b. Indeed, it is well established that NO_x production from reciprocating engines increases with the working load, hence part-loads of DF and NG engines are frequently imposed by the energy management system in Fig. 6c.

Focusing the attention on cost optimization, Fig. 6d reports results in terms of electrical power distribution over all the ship operating conditions. It must be remarked that carbon pricing for cost computation is here fixed according to short-term scenarios commonly foreseen for Europe [52]. Comparing Fig. 6d with Figs. 6a and 6b, results obtained for cost optimization appear qualitatively similar to those obtained from the η_g and $CO_{2,eq}$ optimization. Batteries are charged during navigation on the routes Genoa-Civitavecchia, Civitavechia-Palermo and Barcelona-Genoa, as well as during maneuvering in arrival to Genoa. On the other hand, power is withdrawn from electrical energy storage system during maneuvering and few port conditions. However, the main difference introduced by the cost optimization consists in discharging

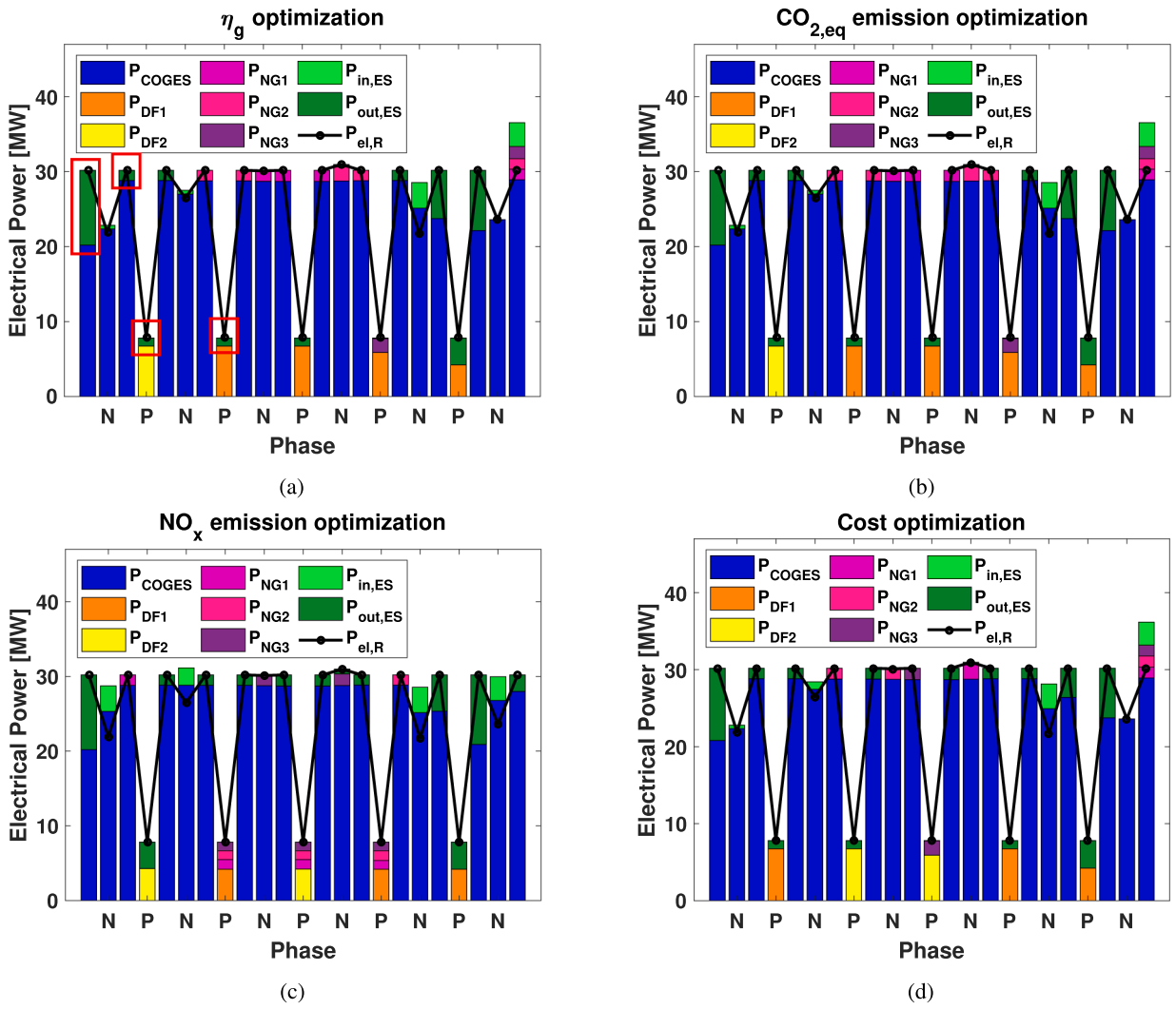

Fig. 6. Electrical power distribution for phase-mean analysis during winter season. Results are optimized for η_g (a), $CO_{2,eq}$ (b), NO_x (c) and costs (d). Costs account for carbon pricing. The subscripts indicate the energy source (COGES = COmbined Gas Electric and Steam plant; DF = Dual-Fuel engines; NG = Natural Gas engines; ES = Energy Storage; R = requested), together with the identification number of the prime mover considered to distinguish between multiple reciprocating engines installed onboard.

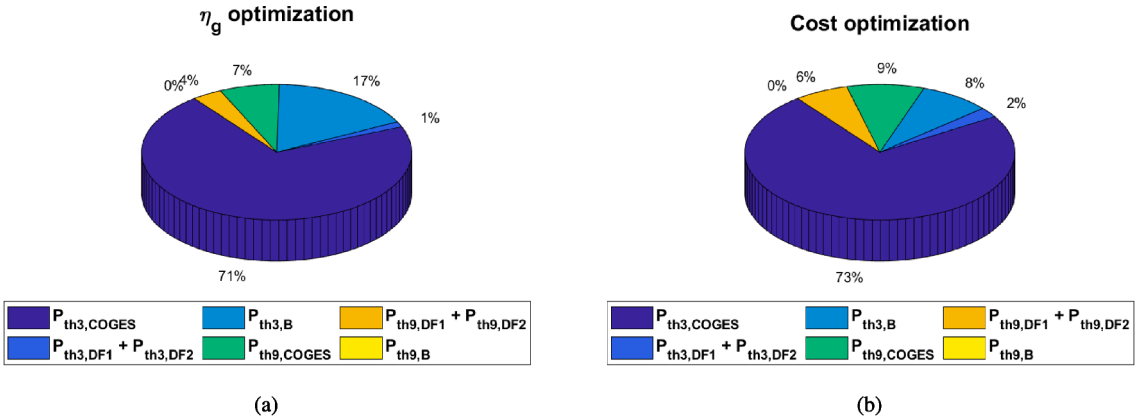

Fig. 7. Cumulative LT and HT thermal power distribution for phase-mean analysis during winter season, for η_g (a) and cost (b) optimizations.

batteries during navigation on the Palermo-La Valletta route instead of during port conditions at Palermo and La Valletta. This occurs due to the trade-off between OPEX cost provided by DF and NG engines and the investment cost of batteries. Indeed, where the sizing of the energy storage system is concerned, the optimization processes of η_g, $CO_{2,eq}$ and NO_x all agree to size battery pack to 40000 kWh, which corresponds to 2000 batteries developing 20 kWh each. Instead, cost minimization is achieved by adopting a 37640 kWh capacity. This slightly different

Table 6
Objective function values obtained for all the optimization procedures considered, during the 8-days phase-mean profile. Analogous results computed for a reference power plant (Ref) without batteries installed are also reported for comparison.

CONFIGURATION		η_g	$CO_{2,eq}$ [t]	NO_x [t]	Cost [k€]	Ref
η_g optimization	W	83.05	1792.8	3.090	549.22	$\eta_g = 81.8$
	S	78.35	1760.8	1.991	534.72	$\eta_g = 77.2$
$CO_{2,eq}$ optimization	W	83.05	1792.8	3.090	549.22	$CO_{2,eq} = 1822.0$
	S	78.35	1760.8	1.991	534.72	$CO_{2,eq} = 1809.8$
NO_x optimization	W	82.05	1808.6	2.920	552.32	$NO_x = 3.272$
	S	78.04	1766.4	1.952	535.84	$NO_x = 2.762$
Cost optimization	W	83.03	1793.1	3.082	549.12	Costs = 549.22
	S	78.34	1761.0	1.966	534.41	Costs = 538.71

LT thermal power delivered by DF engines only represents 1–2% of the overall thermal power demand. Focusing on the HT thermal power demand, most of the steam at 9 bar is provided by the spillage from the steam turbine included in COGES plant, whereas DF engines cover about half of it. On the other hand, no boiler for generating 9 bar steam is required, since waste heat from prime movers manages to cover demand in all the ship operating conditions. The relevance of reciprocating engines in HT thermal power production appears to mainly derive from the amount of steam at 9 bar usually required for laundry, galley and propulsion auxiliaries.

In order to provide a detailed view of the values assumed by the objective functions under various optimization strategies, Table 6 summarises cogeneration efficiency, $CO_{2,eq}, NO_x$ and costs obtained from all the phase-mean energy management methodologies, during the 8-days cruise analysed, in summer and winter seasons. Furthermore, also results concerning power plant based on the same prime movers but not including Li-ion battery pack onboard are reported with the aim of clearly visualize pros/cons offered by hybrid-electric configurations. As can be seen, the maximum value for η_g and the minimum values for $CO_{2,eq}, NO_x$ and costs are obtained by its dedicated optimization procedure for both seasons. According to Fig. 6, differences in NO_x emissions from prime movers and in CO_2 emission factors appear negligible, hence results from η_g optimization algorithm coincide with those derived by minimizing $CO_{2,eq}$. Overall, since similar size of energy storage system is identified by all the analyses, weak differences (≈1–2%) arise between the four optimization procedures in terms of cogeneration efficiency and $CO_{2,eq}$, for a fixed season. On the other hand, larger variations between algorithms are obtained in terms of NO_x emissions, where nearly 6% gaps arise. Finally, the choice of objective function affects costs within 2%.

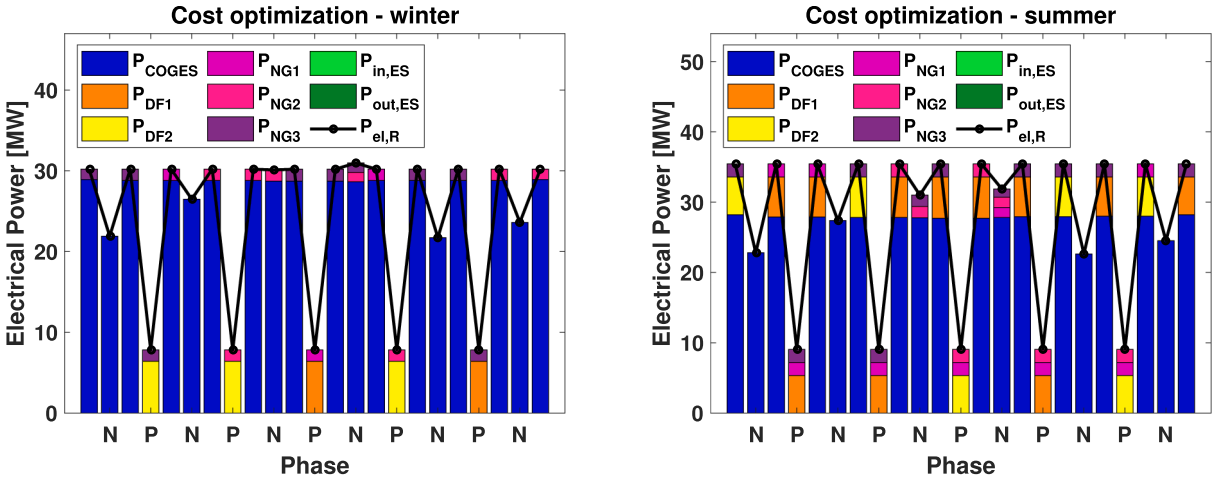

Fig. 8. Electrical power distribution for phase-mean analysis obtained from cost optimization without carbon tax, for winter (a) and summer (b) seasons.

sizing of the EES motivates differences arising between Fig. 6d and Figs. 6a, 6b. Results show that the larger the battery pack the higher the performance of power plant by thermodynamic and environmental points of view, since reduced emissions and fuel consumption may be obtained. On the other hand, the current battery price (i.e. 200 €/kWh) determines a minimum for costs before reaching the maximum size available for batteries. Similarly, capacities exceeding 40 MWh will be economically feasible in future for further reduced investment cost of batteries. Interestingly, results concerning EES sizing based on cost optimization appear well fitted with current projects financed by major shipowners to construct hybrid-electric cruise ships in the last few years [80].

To evaluate the contribution of each prime mover to cover thermal power demands by means of waste heat recovery from exhaust gas, Fig. 7 shows the phase-mean distribution of the LT and HT power supplies onboard. Only results from η_g and cost optimizations are shown in cumulative form for winter season, for the sake of conciseness. As can be seen, independently from the optimization algorithm, most of the LT demand is covered by steam generated by COGES plant (71–73% of the overall thermal power demand), while a significant residual part (i.e. 8–17%) is covered by dedicated auxiliary boilers. Since the waste heat available from reciprocating engines is far lower than that from COGES,

Comparing performances obtained by power plant not including batteries with those available from hybrid-electric configurations, benefits offered by batteries on $\eta_g, CO_{2,eq}, NO_x$ and costs are clearly shown. Specifically, when power plant is equipped with batteries, the energy management system can flexibly move power from/to electrical storage, hence globally increasing prime mover loads during cruise. This results in reduced environmental impact as well as in more efficient energy usage onboard. On the other hand, benefits in terms of cost can be achieved by hybrid-electric propulsion plants if carbon pricing, which will be probably enacted in the early future in Europe, is present.

In order to gain a detailed insight into the outcomes of the phase-mean analysis, the importance of carbon pricing in improving the eco-

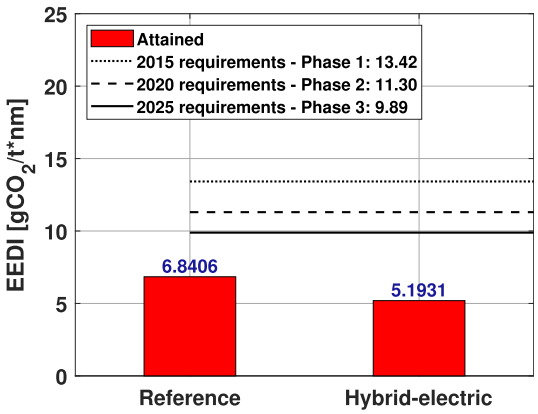

Fig. 9. Energy Efficiency Design Index (EEDI) computed for both reference power plant without any battery installed and hybrid-electric plant.

nomic competitiveness of batteries has been investigated by performing a cost optimization without CO_2 taxation. Results obtained for summer and winter seasons are reported in Fig. 8 in terms of electrical power distribution over all the prime movers included within the engine room. As can be seen, no power exchanged by batteries in charge or discharge modes is visible in Fig. 8. Specifically, comparing Fig. 8 with Fig. 6d, COGES plant, DF and NG engines appear to locally work on higher or lower loads, in order to match electrical power demand without any contribute from batteries. Thus, since in this section optimal sizing of electrical energy storage is additionally performed assuming variable number of batteries, costs result minimized by avoiding battery installation onboard. Therefore, benefits in terms of lower fuel consumption costs available from batteries (see Fig. 6d above) are not able to balance investment costs for electrical energy storage in absence of carbon pricing. This finding well agrees with the policies on carbon pricing in the maritime sector, which will be enacted in the early future in the EU [48,47,49].

Overall, the analyses on phase-mean profiles carried out in this section clearly show how, for the present case study, a 40 MWh energy storage system optimizes power plant performance from energy and environmental point of views. Since energy transition in the maritime sector will require even more strict regulations limiting emissions and promoting energy savings, a 40 MWh capacity will be considered in the following. Nevertheless, with a 200 €/kWh Li-ion battery price, economic optimization provides a slightly different sizing for the energy storage system (37640 kWh). Furthermore, battery price reduction forecast during 2020–2030 will make economically feasible energy storage system dealing with increasingly high sizes for cruise ships [52,81,59].

Finally, in order to clearly assess compliance with recent environmental regulations from IMO, Fig. 9 shows the Energy Efficiency Design Index (EEDI) for the hybrid-electric power plant equipped with 40 MWh battery pack, together with results obtained from the power plant not including batteries onboard. Black lines represent the EEDI required values for cruise ships dealing with non conventional power plants, at the three successive phases introduced by IMO to limit CO_2 emissions. As can be seen, both power plants comply with IMO regulations up to 2025. Specifically, the LNG-fuelled power plant without any energy storage system installed onboard provide EEDI value in agreement with results available from the literature concerning highly efficient cruise ships [82]. However, power plant equipped with batteries provides further reduced EEDI, hence it appears more preferable in an energy transition scenario in view of more stringent limits.

4.2. Optimization procedures applied to hourly demand profiles

In this section, the optimal operation of hybrid-electric power plant equipped with 40 MWh Li-ion battery pack is investigated considering hourly power requests for an overall time extension of 48 h. Details in terms of locations, duration and ship speeds accounted for within the part of the route considered for the hourly analysis are reported in Table 7. Specifically, the power plant operation is optimized by energy, environmental and economic perspectives assuming the four objective functions introduced in Section 2 and focusing on a more detailed time trace. As was above, each optimization is carried out considering thermal and electrical power demands for both summer and winter seasons. However, since results for summer are qualitatively analogous, only winter season is considered for sake of conciseness.

Table 7
Details of the hourly profile considered in Section 4.2 (N = navigation, P = port, M = maneuvering).

LOCATION	PHASE	t [h]	V_{ship} [knots]
Genoa	M	0.5	0
Genoa-Civitavecchia	N	13	15
Civitavecchia	M	0.5	0
Civitavecchia	P	10	0
Civitavecchia	M	0.5	0
Civitavecchia-Palermo	N	15	17
Palermo	M	0.5	0
Palermo	P	7	0
Palermo	M	0.5	0
Palermo-Malta	N	0.5	18

Where the analysis based on hourly profiles is concerned, Fig. 10 shows the electrical power delivered by prime movers in case of η_g (Fig. 10a), $CO_{2,eq}$ (Fig. 10b), NO_x (Fig. 10c) and cost (Fig. 10d) optimizations. The power demand is depicted in black, dotted line, whereas the x-axis indicates time in hours. Since results for summer are qualitatively analogous, only results concerning winter are reported.

Focusing the attention on the η_g optimization (Fig. 10a), approximately 8 MW electrical power is withdrawn from the energy storage in the departure maneuvering from both Genoa and Civitavecchia ports, as well as during the first stages of navigation over the Genoa-Civitavecchia and Civitavecchia-Palermo routes. The rest of electrical power demand during maneuvering and navigation conditions is covered by COGES plant, since it guarantees higher efficiency in comparison to reciprocating engines. Interestingly, where port conditions are concerned, COGES plant is turned on by the optimizer for 50–65% of the time spent at berth, differently from what observed in Section 4.1 for phase-mean power demands. Since power demand at berth is far lower than the minimum load COGES can work at (i.e. 50%, corresponding to 16.51 MW), power delivered by COGES during port conditions is used also to charge batteries, with consequent benefits in terms of cogeneration efficiency in comparison to turning on reciprocating engines. The rest of electrical power demand required during port conditions is provided by batteries or batteries mixed with DF engines. Therefore, electrical energy storage appears to be operated with a mixed spinning-reserve and peak-shaving strategy in combination with COGES: especially when the energy demand is low, excess power is delivered by COGES to charge batteries and increases efficiency of power plant (spinning-reserve); on the other hand, energy is withdrawn from batteries when the power demand is high or particularly low (peak-shaving). Thus, peaks in demand are locally shaved (see red circles in Fig. 10a) and power delivered by COGES is levelized.

Overall, comparing phase-mean with hourly results, COGES plant evidently appears to be turned on more frequently in the second case. Specifically, COGES plant is almost the only prime mover working to maximize efficiency over the 48 h considered, independently from maneuvering, navigation and port conditions. On the other hand, reciprocating engines are turned on over less than 30% of the time spent at berth. This appears due to the higher cogeneration efficiency provided by COGES in comparison to reciprocating engines, with further benefits

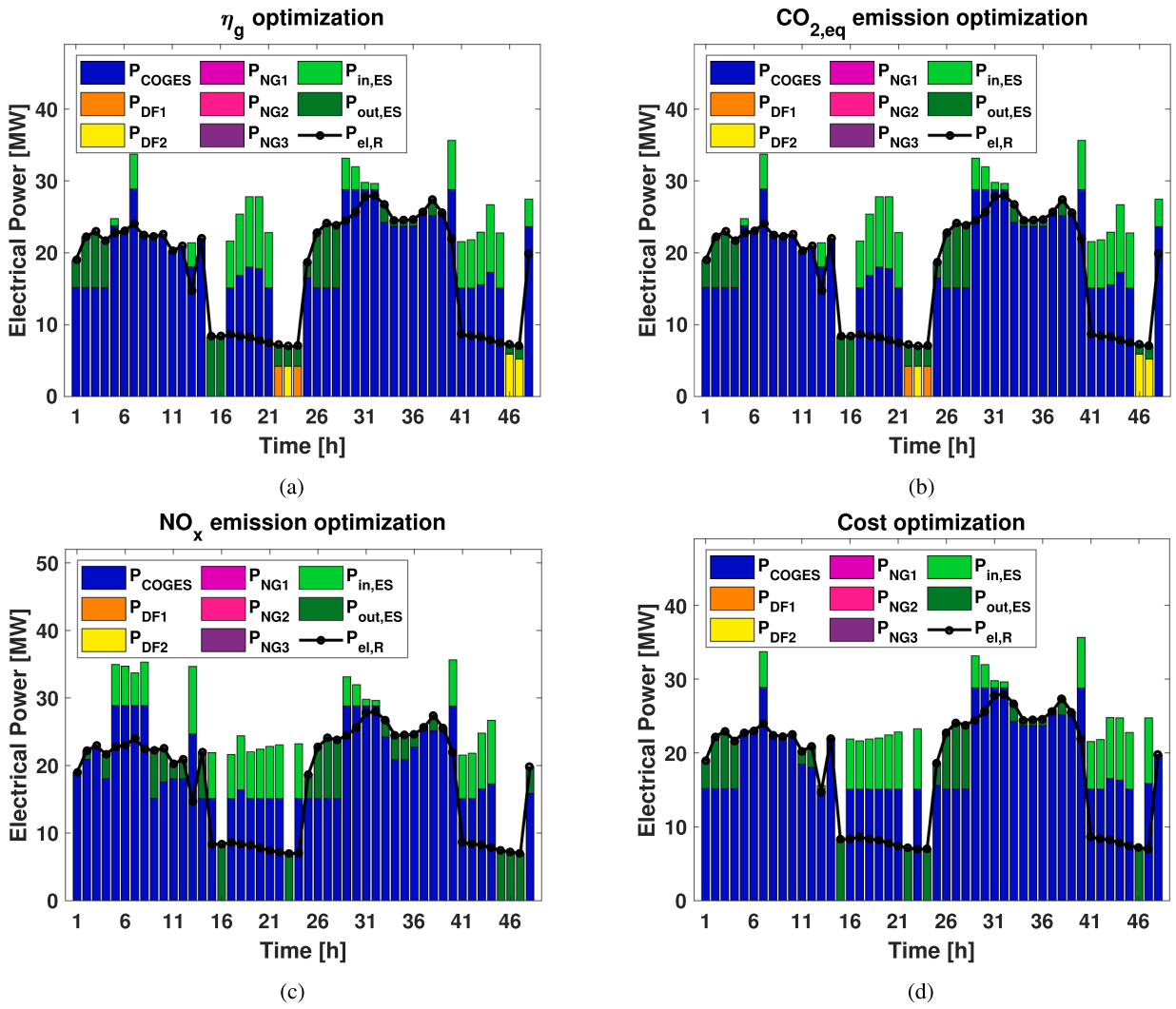

Fig. 10. Electrical power distribution for hourly demand analysis during winter season. Results are optimized for η_g (a), $CO_{2.eq}$ (b), NO_x (c) and costs (d).

provided by synergies with batteries.

Focusing the attention on Fig. 10b, results coincide with those obtained in Fig. 10a. Thus, minimizing equivalent carbon dioxide emissions coincides with the maximization of cogeneration efficiency, as was found in the previous section.

Instead, in case NO_x emissions are required to be minimized (see Fig. 10c), power distribution provided by the optimization process locally differs from results obtained by η_g and $CO_{2.eq}$ optimization algorithms. Specifically, the mixed peak-shaving and spinning-reserve strategy remains the main operating condition of batteries coupled with COGES plant, whereas reciprocating engines are not turned on over the entire 48 h. This directly derives from the far lower NO_x power specific emission guaranteed by COGES (0.22 g/kWh) in comparison to DF or NG engines (3.4 g/kWh). Thus, COGES plant works coupled with batteries in charging or discharging mode over the entire port conditions.

Focusing the attention on cost optimization (Fig. 10d), similarly to Fig. 10c, no reciprocating engines are turned on during all the 48 h, hence COGES coupled with charging/discharging batteries covers power demand also at berth. This behaviour appears to derive from the detailed information concerning hourly power demands, which increases flexibility in distributing load between prime movers and batteries to minimize OPEX costs. In case the energy demand is low, excess power is delivered by COGES to charge batteries and increase efficiency of power plant, as well as energy is withdrawn from batteries when the power demand is high or particularly low. Thus, peak-shaving and spinning-reserve continue to constitute the main energy management strategy.

In order to assess the contribution of each prime mover to cover hourly thermal power requests via waste heat recovery from exhaust gas, results concerning the LT and HT power supplies are shown in Fig. 11, for the winter season. Only results obtained from the η_g and cost optimizations are shown for sake of conciseness. Where the LT power is concerned (top row), COGES plant covers almost the 75–80% of the demand onboard, whereas the remaining part is supplied by auxiliary boilers. Specifically, waste heat recovery from COGES guarantees the base load, whereas auxiliary boilers are used to cover peaks of thermal power demand occurring at morning and evening. Few MWs are provided by DF engines only for the η_g optimization, during port conditions.

Focusing on diagrams for the HT power, Figs. 11c and 11d show how most of the steam at 9 bar required onboard is supplied by the COGES plant, independently from the objective function considered. Where η_g optimization is concerned, DF engines cover the HT demand within the limited time they are turned on at berth, while auxiliary boilers producing steam at 9 bar are enabled for the rest of port conditions.

Therefore, Figs. 10 and 11 globally prove the benefits Li-ion battery pack can offer onboard cruise vessels, by energy, environmental and economic points of view. Specifically, the potential of governing COGES

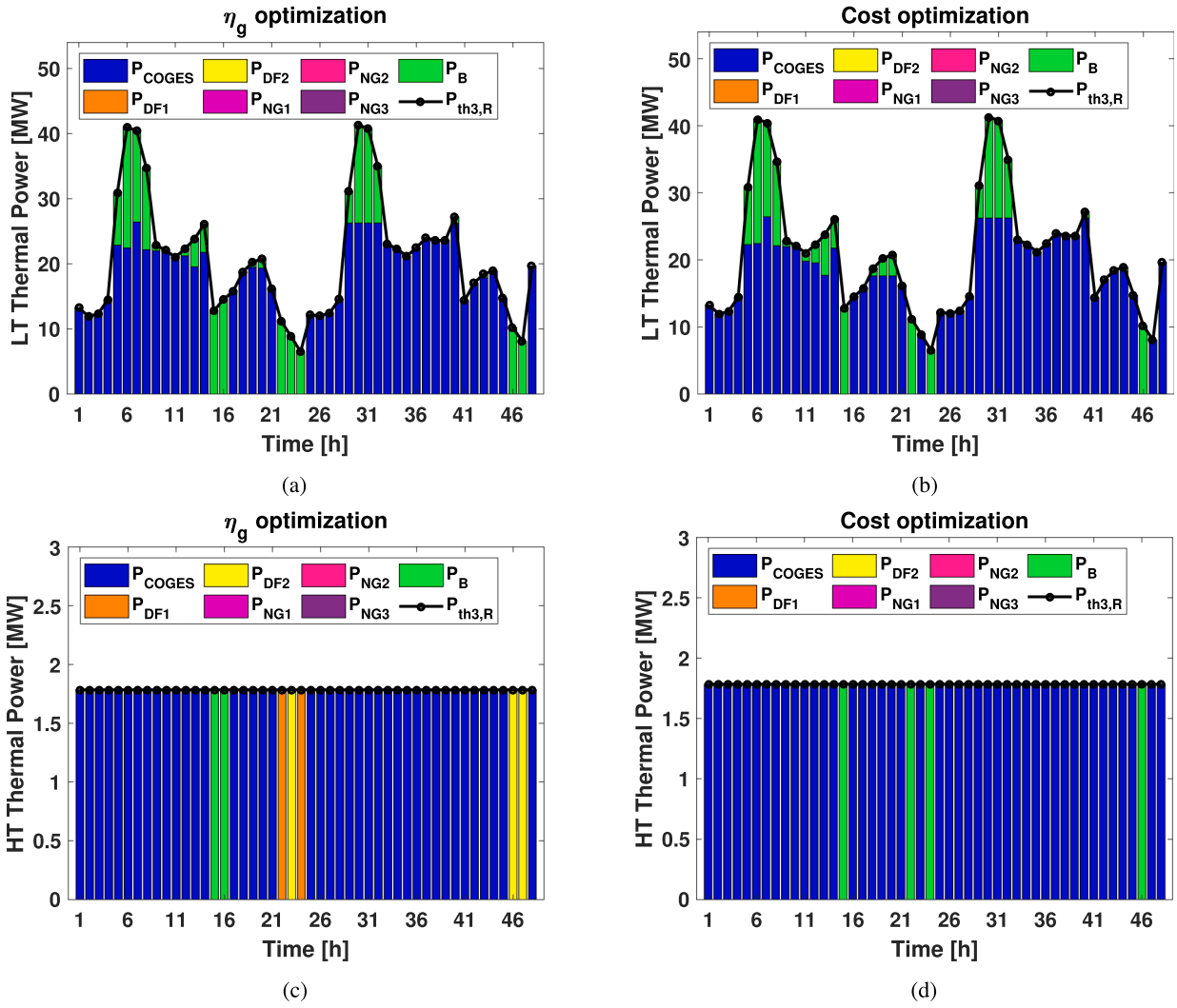

Fig. 11. LT thermal power distribution for hourly demand analysis during winter season, for η_g (a) and cost (b) optimizations. HT thermal power distribution for phase-mean analysis for η_g (c) and costs (d) optimization.

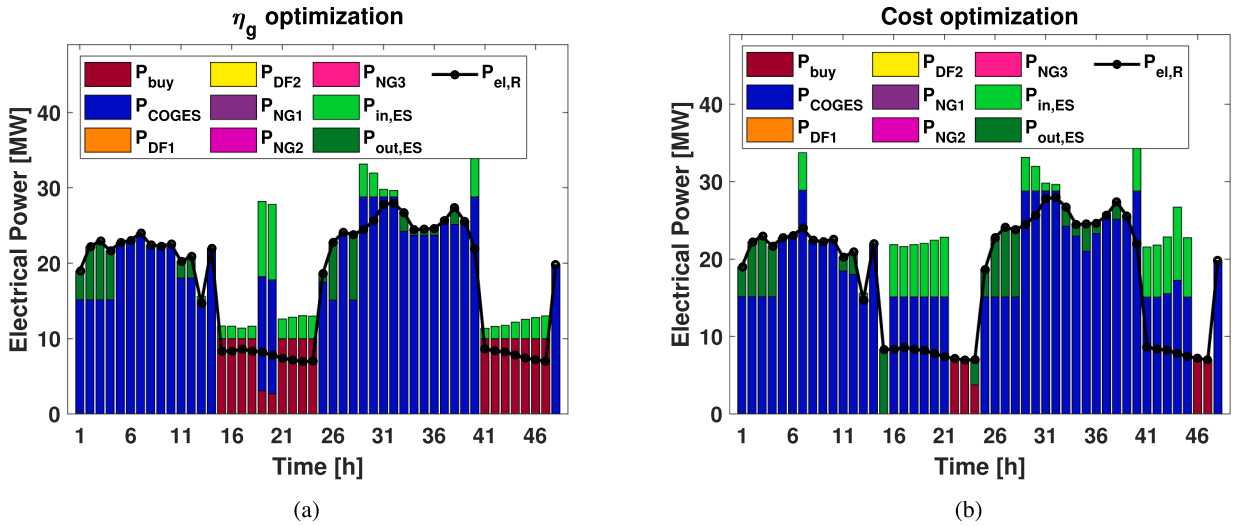

Fig. 12. Electrical power distribution for hourly demand analysis during winter season, considering cold ironing at berth. Results are optimized for η_g (a) and costs (b).

plant and batteries in a mixed peak-shaving and spinning-reserve strategy has been clearly shown. It must be remarked that analyses carried out so far turned on prime movers also during port operating conditions, with no possibilities of cold ironing (CI). However, since CI presently represents one of the main measures considered by port authorities and ownerships to abate emissions when the ships are at berth,

assessing changes in energy management system when cold ironing is available appears relevant. Towards this end, Fig. 12 shows the electrical power distribution during winter, considering an electricity price of 0.065 €/kWh for cold ironing [83,54–56]. Only results from the η_g and cost optimization algorithms are reported for sake of conciseness. Similarly to Fig. 10a, Fig. 12a shows energy withdrawn from batteries during the departure maneuvering from the Genoa and Civitavecchia ports, as well as during the first stages of navigations over the Genoa-Civitavecchia and Civitavecchia-Palermo routes. On the contrary, major differences between Figs. 12a and 10a arise during port conditions, when most of the power request is covered by cold ironing with no role played by DF engines. COGES plant locally delivers power at berth and contributes to charge batteries, though most of power is stored into the energy storage system by the port grid. Little changes between Figs. 12a and 10a also occur during navigation and maneuvering. Indeed, different amounts of energy are stored in batteries during port between Figs. 12a and 10a, hence CI globally influences the energy management strategy. Mixed peak-shaving and spinning-reserve strategy still represents the main governing method for power plant, despite CI availability at berth significantly influences it.

Analogous results can be obtained from the minimization of $CO_{2,eq}$ and NO_x emissions, hence energy and environmental benefits of cold ironing seem well defined. Focusing attention on Fig. 12b, minimizing costs appears to reduce power delivered by cold ironing during port conditions. Indeed, most of the electrical power demand when the vessel is at berth as well as the entire charging of batteries at ports are supplied by COGES plant, similarly to what obtained in Fig. 10d. This clearly shows how costs for maintenance and fuel consumption related to high-load operating conditions of COGES plant are lower than expense for cold ironing. Furthermore, COGES coupled with batteries entirely cover power demand during navigation and maneuvering. Overall, the mixed peak-shaving and spinning-reserve strategy dominates the electrical energy storage system operation: power is withdrawn from batteries during highly demanding conditions, whereas charging mode is used to increase the load of COGES plant, when the electrical power demand is lower.

Investigations considering cold ironing confirm the benefits provided by batteries onboard cruise ships and underline how CI is economically competitive with COGES plant, despite its viability may be improved. Furthermore, the optimal energy management strategy remains mixing peak-shaving and spinning-reserve, with minor differences concerning prime mover loads.

5. Conclusions

In this work, the energy, environmental and economic performances provided by hybrid-electric power plants installed onboard large-size cruise vessels have been investigated.

First, the optimal operation of power plant has been assessed focusing on phase-mean electrical and thermal power demands. Independently from the objective function considered, most of the power demands onboard during navigation and maneuvering resulted to be covered by COGES, whereas reciprocating engines were only turned on during port activities. On the other hand, power is withdrawn from batteries during maneuvering and port, whereas charging mode takes place within navigation. Overall, batteries are shown to promote lower EEDI and flexible energy management, with consequent benefits in comparison to non hybrid-electric power plant. Specifically, within energy and environmental optimization studies, both charging and discharging modes of batteries enable benefits in terms of η_g and $CO_{2,eq}$ emissions by increasing the working load of prime movers. On the other hand, economic competitiveness of batteries currently resulted to be deeply influenced by the presence of carbon pricing, which will be enacted in Europe within few years. Overall, 40 MWh resulted to be the optimal sizing of battery pack by energy and environmental perspectives, with weak difference obtained from the economic optimization.

Successively, hourly profiles have been considered to provide a detailed insight into optimal schedules of hybrid-electric power plant dealing with 40 MWh electrical energy storage system. Results showed the great potential of combining COGES plant with batteries onboard cruise ships. Specifically, independently from the objective function considered, almost the entire amount of power demand onboard resulted to be supplied by COGES coupled with charging/discharging batteries, following a mixed peak-shaving and spinning-reserve strategy. In detail, when the energy demand is low, excess power is delivered by COGES to charge batteries, while energy is withdrawn from the storage system when the power demand is high or particularly low. Reciprocating engines effectively contribute to power balance only for 30% of time spent at berth when η_g maximization or CO_2 minimization are targeted. In case cold ironing is available at berth, the mixed peak-shaving and spinning-reserve operating mode for COGES and batteries still dominates, though the grid covers significant portion of power demand during port, especially under energy and environmental optimization.

CRediT authorship contribution statement

A. Dotto: Conceptualization, Data curation, Investigation, Methodology, Software, Visualization, Writing - original draft, Writing - review & editing. **F. Satta:** Supervision, Writing - review & editing.

6. Appendix

Constraints setting up the engine room configuration:

$$\begin{aligned} x^{G}_{g,t} &\leqslant y^{G}_{g,t} \\ x^{R}_{r,t} &\leqslant y^{R}_{r,t} \\ x^{B3}_{b,t} &\leqslant y^{B3}_{b,t} \\ x^{B9}_{b,t} &\leqslant y^{B9}_{b,t} \end{aligned} \tag{6}$$

Constraints imposing minimum and maximum values for electrical and thermal power of prime movers as well as boilers:

$$\begin{aligned} &\pi^{el,G}_{g} \leqslant P^{G}_{el,g,t} \leqslant \Pi^{el,G}_{g} \;||\; P^{G}_{el,g,t} = 0 \\ &\pi^{th3,G}_{g} \leqslant P^{G}_{th3,g,t} \leqslant \Pi^{th3,G}_{g} \;||\; P^{G}_{th3,g,t} = 0 \\ &\pi^{th9,G}_{g} \leqslant P^{G}_{th9,g,t} \leqslant \Pi^{th9,G}_{g} \;||\; P^{G}_{th9,g,t} = 0 \\ &\pi^{el,R}_{r} \leqslant P^{R}_{el,r,t} \leqslant \Pi^{el,R}_{r} \;||\; P^{R}_{el,r,t} = 0 \\ &\pi^{th3,R}_{r} \leqslant P^{R}_{th3,r,t} \leqslant \Pi^{th3,R}_{r} \;||\; P^{R}_{th3,r,t} = 0 \\ &\pi^{th9,R}_{r} \leqslant P^{R}_{th9,r,t} \leqslant \Pi^{th9,R}_{r} \;||\; P^{R}_{th9,r,t} = 0 \\ &\pi^{B3}_{b} \leqslant P^{B3}_{b,t} \leqslant \Pi^{B3}_{b} \;||\; P^{B3}_{b,t} = 0 \\ &\pi^{B9}_{b} \leqslant P^{B9}_{b,t} \leqslant \Pi^{B9}_{b} \;||\; P^{B9}_{b,t} = 0 \\ &c^{el,ES} \leqslant P^{ES}_{in,t} \leqslant C^{el,ES} \\ &d^{el,ES} \leqslant P^{ES}_{out,t} \leqslant D^{el,ES} \\ &\pi_{grid} \leqslant P_{grid,t} \leqslant \Pi_{grid} \end{aligned} \tag{7}$$

Constraints imposing piecewise linearization of efficiency and fuel consumption curves for COGES and reciprocating engines [68,69]:

$$\begin{aligned} \eta^{G}_{g,t} &= \mu^{G}_{g,t} P^{G}_{el,g,t} + \tau^{G}_{g,t} \\ \eta^{R}_{r,t} &= \mu^{R}_{r,t} P^{R}_{el,r,t} + \tau^{R}_{r,t} \\ F^{G}_{g,t} &= \sigma^{G}_{g,t} P^{G}_{el,g,t} + \psi^{G}_{g,t} \\ F^{R}_{r,t} &= \sigma^{R}_{r,t} P^{R}_{el,r,t} + \psi^{R}_{r,t} \end{aligned} \tag{8}$$

Constraints aimed at computing CO_2 and NO_x emissions from COGES, reciprocating engines and boilers:

Constraints aimed at cost computation:

$$
\begin{aligned}
&Em^{G}_{g,t} = F^{G}_{g,t}\gamma^{LNG}_{CO_2}\\
&Em^{R}_{r,t} = F^{R}_{r,t}\gamma^{LNG}_{CO_2} + F^{R}_{r,t}\gamma^{MDO}_{CO_2}\\
&Em^{B3}_{b,t} = F^{B3}_{b,t}\gamma^{MDO}_{CO_2}\\
&Em^{B9}_{b,t} = F^{B9}_{b,t}\gamma^{MDO}_{CO_2}\\
&Emno^{G}_{g,t} = \widetilde{\alpha}^{G}_{NO_x}P^{G}_{el,g,t} + \widetilde{\beta}^{G}_{NO_x}Emno^{R}_{r,t} = \widetilde{\alpha}^{R}_{NO_x}P^{R}_{el,r,t} + \widetilde{\beta}^{R}_{NO_x}Emno^{B3}_{b,t} = \widetilde{\alpha}^{B3}_{NO_x}P^{B3}_{b,t} + \widetilde{\beta}^{B3}_{NO_x}Emno^{B9}_{b,t} = \widetilde{\alpha}^{B9}_{NO_x}P^{B9}_{b,t} + \widetilde{\beta}^{B9}_{NO_x}
\end{aligned}
\tag{9}
$$

$$
\begin{aligned}
&CAPEX^{G}_{g} = CC_{G}P^{G}_{el,0,g}CRF\\
&CAPEX^{R}_{r} = CC_{R}P^{R}_{el,0,r}CRF\\
&CAPEX^{B3}_{b} = CC_{B3}\Pi^{B3}_{b}CRF\\
&CAPEX^{B9}_{b} = CC_{B9}\Pi^{B9}_{b}CRF\\
&OPEX^{G}_{g,t} = CF^{LNG}F^{G}_{g,t} + CM^{G}P^{G}_{el,g,t}\\
&OPEX^{R}_{r,t} = CF^{LNG}F^{R}_{LNG,r,t} + CF^{MDO}F^{R}_{MDO,r,t}\\
&+CM^{R}P^{R}_{el,r,t}\\
&OPEX^{B3}_{b,t} = CF^{MDO}F^{B3}_{b,t} + CM^{B3}P^{B3}_{b,t}\\
&OPEX^{B9}_{b,t} = CF^{MDO}F^{B9}_{b,t} + CM^{B9}P^{B9}_{b,t}\\
&CEM^{G}_{g,t} = CTEm^{G}_{g,t}\\
&CEM^{R}_{r,t} = CTEm^{R}_{r,t}\\
&CEM^{B3}_{b,t} = CTEm^{B3}_{b,t}\\
&CEM^{B9}_{b,t} = CTEm^{B9}_{b,t}\\
&CAPEX^{ES} = C_{bal}CC_{ES}CRF_{ES}\\
&CG_{t} = p_{el}P_{grid,t}
\end{aligned}
\tag{10}
$$

Declaration of Competing Interest

The authors declare that they have no known competing financial interests or personal relationships that could have appeared to influence the work reported in this paper.

Data availability

The data that has been used is confidential.

References

[1] IMO, Report of the marine environment protection committee (mepc) on its fifty-seventh session 57th session.
[2] IMO, International convention for the prevention of pollution from ships (marpol) annex VI.
[3] P. Balcombe, J. Brierley, C. Lewis, L. Skatvedt, A. Speirs, J.and Hawkes, I. Staffell, How to decarbonise international shipping: Options for fuels, technologies and policies, Energy Convers. Manage. 182 (2019) 72–88.
[4] Horvath S, Fasihi M, Breyer C. Techno-economic analysis of a decarbonized shipping sector: Technology suggestions for a fleet in 2030 and 2040. Energy Convers Manage 2018;164:230–41.
[5] Trivyza N, Rentizelas A, Theotokatos G. A novel multi-objective decision support method for ship energy systems synthesis to enhance sustainability. Energy Convers Manage 2018;168:128–49.
[6] Inal OB, Charpentier JF, Deniz C. Hybrid power and propulsion systems for ships: Current status and future challenges. Renew. Sustain. Energy Rev. 2022;156: 111965.
[7] Ancona MA, Baldi F, Bianchi M, Branchini L, Melino F, Peretto A, Rosati J. Efficiency improvement on a cruise ship: Load allocation optimization. Energy Convers Manage 2018;164:42–58.
[8] H. Lan, S. Wen, Y.-Y. Hong, D.C. Yu, L. jun Zhang, Optimal sizing of hybrid pv/diesel/battery in ship power system, Appl Energy 158 (2015) 26–34.
[9] Misyris GS, Marinopoulos A, Doukas DI, Tengnér T, Labridis DP. On battery state estimation algorithms for electric ship applications. Electric Power Syst Res 2017; 151:115–24.
[10] Dedes E, Hudson DA, Turnock SR. Assessing the potential of hybrid energy technology to reduce exhaust emissions from global shipping. Energy Policy 2012; 40:204–18.
[11] G.T.T. Vieira, C.O. Peralta, M.B.C. Salles, B.S. Carmo, Reduction of co2 emissions in ships with advanced energy storage systems, 2017 6th International Conference on Clean Electrical Power (ICCEP) (2017) 564–571.
[12] Geertsma R, Negenborn RR, Visser K, Hopman JJ. Design and control of hybrid power and propulsion systems for smart ships: A review of developments. Appl Energy 2017;194:30–54.
[13] Zahedi B, Norum LE, Ludvigsen KB. Optimized efficiency of all-electric ships by dc hybrid power systems. J Power Sources 2014;255:341–54.
[14] Wang L, Lee DJ, Lee W, Chen Z. Analysis of a novel autonomous marine hybrid power generation/energy storage system with a high-voltage direct current link. J Power Sources 2008;185:1284–92.
[15] Besikçi EB, Arslan Ö, Turan O, Ölçer AI. An artificial neural network based decision support system for energy efficient ship operations. Comput Oper Res 2016;66: 393–401.
[16] MAN, Man 51/60df IMO tier ii, IMO tier iii project guide-marine (2015) 411–414.
[17] L. Smith, H. Karim, S. Etemad, W.C. Pfefferle, The gas turbine handbook, 2006.
[18] Merz C, Pakula T. The design and operational characteristics of a combined cycle marine power plant. *Turbo Expo: Power for Land, Sea* and Air. Am Soc Mech Eng (ASME) 1972:79818.
[19] Haglind F. A review on the use of gas and steam turbine combined cycles as prime movers for large ships. Part ii: Previous work and implications. Energy Convers Manage 2008;49:3468–75.
[20] Benvenuto G, Bertetta D, Campora U, Carollo F. Cogas plant as possible future alternative to the diesel engine for the propulsion of large ships. Sustain Mar Transp Exploitation Sea Resources–Rizzuto & Guedes Soares 2011:13–6.
[21] G. Benvenuto, U. Campora, M. Laviola, Assessment of steam cycle layouts for cogas ship propulsion systems, Proceedings of the 2th International Conference on Maritime Technology and Engineering (2014) 743–754.
[22] Altosole M, Figari M, Viviani M, Michetti S, Trapani A. Simulation of the dynamic behaviour of a codlag propulsion plant. Proceedings WARSHIP 2010 Conference: Advanced Technologies in Naval Design and Construction 2010:109–15.
[23] Altosole M, Benvenuto G, Figari M, Campora U, Bagnasco A, D'Arco S, et al. Real time simulation of the propulsion plant dynamic behaviour of the aircraft carrier cavour. Proceedings INEC 2008.
[24] Dotto A, Campora U, Satta F. Feasibility study of an integrated coges-df engine power plant in lng propulsion for a cruise-ferry. Energy Convers Manage 2021;245: 114602.
[25] Dotto A, Satta F, Campora U. Energy, environmental and economic investigations of cruise ships powered by alternative fuels. Energy Convers Manage 2023;285: 117011.
[26] Dotto A, Sacchi R, Satta F, Campora U. Dynamic performance simulation of combined gas electric and steam power plants for cruise-ferry ships. Next Energy 2023:100020.
[27] Barsi D, Luzzi M, Satta F, Zunino P. On the possible introduction of mini gas turbine cycles onboard ships for heat and power generation. Energies 2021;14(3): 1–12. 568.
[28] Barsi D, Costa C, Satta F, Zunino P, Busi A, Ghio R, Raffaeli C, Sabattini A. Design of a mini combined heat and power cycle for naval applications. J Sustain Develop Energy, Water Environ Syst 2020;8:281–92.
[29] Barsi D, Costa C, Satta F, Zunino P, Sergeev V. Feasibility of mini combined cycles for naval applications. In: MATEC Web of Conferences. vol. 245; 2018. p. 07008.
[30] Weber C, Maréchal F, Favrat D. Design and optimization of district energy systems. Computer-aided Chem Eng 2007;24:1127–32.
[31] Hawkes AD, Leach M. Modelling high level system design and unit commitment for a microgrid. Appl Energy 2009;86:1253–65.
[32] Genon G, Torchio MF, Poggio A, Poggio MA. Energy and environmental assessment of small district heating systems: Global and local effects in two case-studies. Energy Convers Manage 2009;50:522–9.
[33] Domínguez-Muñoz F, Cejudo-López JM, Carrillo-Andrés A, Gallardo-Salazar M. Selection of typical demand days for chp optimization. Energy Build 2011;43(11): 3036–43.
[34] Onovwiona HI, Ugursal VI. Residential cogeneration systems: Review of the current technology. Renew Sustain Energy Rev 2006;10:389–431.
[35] Bracco S, Dentici G, Siri S. Economic and environmental optimization model for the design and the operation of a combined heat and power distributed generation system in an urban area. Energy 2013;55:1014–24.
[36] J.Y. Wu, J. long Wang, S. Li, Multi-objective optimal operation strategy study of micro-cchp system, Energy 48 (2012) 472–483.
[37] Mehleri ED, Sarimveis H, Markatos NC, Papageorgiou LG. A mathematical programming approach for optimal design of distributed energy systems at the neighbourhood level. Energy 2012;44:96–104.
[38] S. Bracco, F. Delfino, F. Pampararo, M. Robba, M. Rossi, Economic and environmental performances quantification of the university of genoa smart

polygeneration microgrid, 2012 IEEE International Energy Conference and Exhibition (ENERGYCON) (2012) 593–598.
[39] Weber C, Shah N. Optimisation based design of a district energy system for an eco-town in the united kingdom. Energy 2011;36(2):1292–308.
[40] Ren H, Gao W. A milp model for integrated plan and evaluation of distributed energy systems. Appl Energy 2010;87:1001–14.
[41] Arya AK. A comparison of the moga and nsga-ii optimization techniques to reduce the cost of a biomass supply network. Mater Today: Proc 2022;57:1553–8.
[42] Bolbot V, Trivyza NL, Theotokatos G, Boulougouris E, Rentizelas A, Vassalos D. Cruise ships power plant optimisation and comparative analysis. Energy 2020;196:117061.
[43] Ghaemi Z, Tran TT, Smith AD. Comparing classical and metaheuristic methods to optimize multi-objective operation planning of district energy systems considering uncertainties. Appl Energy 2022;321:119400.
[44] Pruitt KA, Braun RJ, Newman AM. Evaluating shortfalls in mixed-integer programming approaches for the optimal design and dispatch of distributed generation systems. Appl Energy 2013;102:386–98.
[45] Gabrielli P, Acquilino A, Siri S, Bracco S, Sansavini G, Mazzotti M. Optimization of low-carbon multi-energy systems with seasonal geothermal energy storage: The anergy grid of eth zurich. Energy Convers Manage 2020;8:100052.
[46] Coffrin C, Hentenryck PV. A linear-programming approximation of ac power flows. Informs J Comput 2014;26:718–34.
[47] URL: https://ec.europa.eu/clima/eu-action/eu-emissions-trading-system-eu-ets_it.
[48] URL: https://ec.europa.eu/commission/presscorner/detail/en/qanda_21_3662.
[49] URL: https://ec.europa.eu/clima/eu-action/eu-emissions-trading-system-eu-ets_it?wt-search=yes.
[50] Oo TZ, Ren Y, Kong AW-K, Wang Y, Liu X. Power system design optimization for a ferry using hybrid-shaft generators. IEEE Trans Power Syst 2022;37:2869–80.
[51] Gas turbine world 2012, Pequot Editor (2012).
[52] Perčić M, Vladimir N, Fan A. Life-cycle cost assessment of alternative marine fuels to reduce the carbon footprint in short-sea shipping: A case study of croatia. Appl Energy 2020;279:115848.
[53] Lammel G, Grassl H. Greenhouse effect of NOx. Environ Sci Pollut Res 1995;2:40–5.
[54] Martínez-López A, Romero-Filgueira A, Chica M. Specific environmental charges to boost cold ironing use in the european short sea shipping. Transp Res Part D-Transp Environ 2021;94:102775.
[55] E. Korn, The maritime commons: Digital repository of the world maritime university chapters library 2009 scatterplots with survey data, 2017.
[56] Wilske A. Examining the commercial viability of cold ironing. Port of Gothenburg 2010.
[57] Livanos G, Theotokatos G, Pagonis D. Techno-economic investigation of alternative propulsion plants for ferries and roro ships. Energy Convers Manage 2014;79:640–51.
[58] Perčić M, Frković L, Pukšec T, Ćosić B, Li OL, Vladimir N. Life-cycle assessment and life-cycle cost assessment of power batteries for all-electric vessels for short-sea navigation. Energy 2022;251:123895.
[59] Lehmusto M, Santasalo-Aarnio A. Mathematical framework for total cost of ownership analysis of marine electrical energy storage inspired by circular economy. J Power Sources 2022;528:231164.
[60] Perčić M, Vladimir N, Fan A. Techno-economic assessment of alternative marine fuels for inland shipping in croatia. Renew Sustain Energy Rev 2021;148:111363.
[61] Perčić M, Ančić I, Vladimir N. Life-cycle cost assessments of different power system configurations to reduce the carbon footprint in the croatian short-sea shipping sector. Renew Sustain Energy Rev 2020;131:110028.
[62] Maddaloni JD, Rowe A, van Kooten GC. Wind integration into various generation mixtures. Renewable Energy 2009;34:807–14.
[63] L. Davis, S. Black, Dry Low Nox Combustion Systems for GE Heavy-Duty Gas Turbines, GE Power Systems Schenectady, NY, GER-3568G.
[64] Verbeek R, Kadijk G, Van Mensch P, Wulffers C, Van Den Beemt B, Fraga F, Aalbers A. Environmental and Economic aspects of using LNG as a fuel for shipping in The Netherlands. Delft: TNO; 2011.
[65] Armellini A, Daniotti S, Pinamonti P. Gas turbines for power generation on board of cruise ships: A possible solution to meet the new imo regulations? Energy Procedia 2015;81:540–7.
[66] IMO, Energy efficiency for cruise passenger ships, International Maritime Organization, MEPC 65/4/6.
[67] IMO, Resolution mepc.212(63) guidelines on the method of calculation of the attained energy efficiency design index (eedi) for new ships, MEPC 63/23, London: International Maritime Organization.
[68] Fourer R. A simplex algorithm for piecewise-linear programming i: Derivation and proof. Math Program 1985;33:204–33.
[69] Goldberg N, Rebennack S, Kim Y, Krasko V, Leyffer S. Minlp formulations for continuous piecewise linear function fitting. Comput Optim Appl 2021;79:223–33.
[70] Winnes H, Fridell E. Particle emissions from ships: dependence on fuel type. J Air Waste Manage Assoc 2009;59(12):1391–8.
[71] Winnes H, Fridell E, Yaramenka K, Nelissen D, Faber J, Ahdour S. NOx controls for shipping in eu seas. Swedish Environmental Research Institute; 2016.
[72] Gualeni P, Boveri A, Silvestro F, Margarita A. Decision support system for power generation management for an 110000+ grt cruise ship. Int J Maritime Eng. 2016.
[73] Meyer P, Maes F, Volckaert A. Emissions from international shipping in the belgian part of the north sea and the belgian seaports. Atmos Environ 2008;42:196–206.
[74] Tzannatos E. Ship emissions and their externalities for the port of piraeus - greece. Atmos Environ 2010;44:400–7.
[75] Amaya-Vías D, Nebot E, López-Ramírez JA. Comparative studies of different membrane distillation configurations and membranes for potential use on board cruise vessels. Desalination 2018;429:44–51.
[76] Gnes P, Pinamonti P, Reini M. Bi-level optimization of the energy recovery system from internal combustion engines of a cruise ship. Appl Sci 2020;10:6917.
[77] Baldi F, Ahlgren F, Nguyen T-V, Thern M, Andersson K. Energy and exergy analysis of a cruise ship. Energies 2018;11:2508.
[78] Baldi F, Ahlgren F, Melino F, Gabrielii CH, Andersson K. Optimal load allocation of complex ship power plants. Energy Convers Manage 2016;124:344–56.
[79] G. DNV, Guidance for safe return to port projects', Class Guideline, DNVGL-CG 4.
[80] URL: https://www.carnivalcorporation.com/news-releases/news-release-details/aidaperla-will-receive-largest-battery-storage-system-passenger/.
[81] Tsiropoulos I, Tarvydas D, Lebedeva N. Li-ion batteries for mobility and stationary storage applications – scenarios for costs and market growth. Publications Office of the European Union; 2018.
[82] Trivyza NL, Rentizelas AA, Theotokatos G. A comparative analysis of eedi versus lifetime co2 emissions. J Mar Sci Eng 2020;8:61.
[83] A. Abdaoui, Feasibility study of cold ironing from renewable sources in the nordic region: case study: Port of Kapellskär in Stockholm, 2022.